UNIVERSIDADE DA BEIRA INTERIOR
Ciências da Saúde

Neuroinflammation and neurogenesis in the choroid plexus

Nádia Patrícia Amaral Morete

Dissertação para obtenção do grau de mestre em
Ciências Biomédicas
(2º Ciclo de estudos)

Orientador: Professora Doutora Cecília Santos
Coorientador: Mestre Joana Tomás

Covilhã, outubro de 2014

"The price of success is hard work, dedication to the job at hand, and the determination that whether we win or lose, we have applied the best of ourselves to the task at hand."

Vince Lombardi

Acknowledgments

It is extremely difficult to express all my gratitude, my feelings, my respect and also my deep admiration to all of you that during these five years in Covilhã, directly or indirectly, help me along my way. I just want to say thanks for everything!

To Cecília Santos, I wish to express my sincere thanks for your scientific support, for your supervision, for your constructive criticism. I wish to express my sincere and honest thanks for the opportunity to work in your group research.

To Joana Tomás I want to express my thankfulness. More than a supervisor she was my "research mother" with whom I had learn not only, I hope, to be a good scientist, but also to be a simple human being always ready to chase my dreams without giving up.

To Graça Baltazar and Liliana Bernardino, I would like to thank for all the scientific and logistic support provided.

Also, I thanks to the entire lab group, "Neurons & Neurons", for their friendship, thank you for helpful advice and a great work environment.

I thanks to my friends, especially Ana Sofia, Raquel, Telmo, and Lena for their brotherhood, I spent some of the best moments of my life with you!! Thanks for your friendship, for always being there.

And the most importantly, I would also like to express my sincere thanks to my parents. Thanks for the unconditional support and for always believing in me when I doubted myself. Thank You, thank You, thank you!!! I love you more than myself.

And last, thank you, God.

Abstract

The choroid plexus (CP), located within the cerebral ventricles, are composed of a highly vascularized stroma surrounded by a tight layer of epithelial cells that restrict cellular and molecular traffic between the blood and the cerebrospinal fluid (CSF). Stroma is surrounded by dendritic cells, collagen fibbers, fibroblasts and B and T cells. Some of these cells are innate immune cells whose main function is antigen presentation which suggest that CP may play an active role in immunological brain protection. CP can be seen as a first line of defense in brain against harmful stimulus, whether they are molecules, cells or pathogens, due to the presence of tight junctions (TJ). TJ control the paracellular permeability across lateral intracellular spaces preventing solutes and water from passing freely through the paracellular pathway and form a boundary between the apical and basolateral plasma membrane domains by preventing diffusion of proteins between the membrane compartments. On the other hand, recent studies suggest that the CP cells can differentiate into neurons and astrocytes. So we proposed to evaluate the effect of an acute neuroinflammatory insult, lipopolysaccharide (LPS), in CP neurogenesis. The reactive oxygen species (ROS) and nitric oxide (NO) production alterations in protein content of extracellular medium was analyzed *in vitro* with the establishment of a primary culture of choroid plexus epithelial cells (CPEC). The inflammatory response of CP to LPS was analyzed *in vivo* in C57BL/6 mice injected with LPS and sacrificed 7h after and *ex vivo* in CP explants from newborn rats incubated with LPS. For that we studied neuroinflammatory markers such as: CD11b, a microglia marker; NeuN, a mature neurons marker and GFAP, an astrocytes marker, by the whole mount technique. We also studied the effect of LPS in CP integrity as a barrier by studying the differential expression of TJ proteins. The effect of LPS in Occludin, E-cadherin, ZO-1 and claudin-1 expression was quantified *in vitro* by immunocytochemistry (ICC), occludin and E-cadherin expression was also analyzed *ex vivo*, by whole mount and *in vivo* by Western blot. LPS triggered an increase in ROS production, NO and in total protein content of extracellular medium in CPEC. The neuroinflammatory response of CP to LPS resulted in an over expression of CD11b and GFAP, a decrease in NeuN expression but no changes in TTR expression were observed. Our findings suggest an increase in iNOS production. Lastly, we observed that CP kept its barrier proteins despite minor alterations in occludin expression. In conclusion, the work developed shows that CP responded to acute neuroinflammation by increasing the expression of proteins involved in immunological brain protection. Morphologically CP keeps its integrity as a barrier but the alteration on proteins that encode TJ indicates that a disturbance on this CP function may be compromised.

Keywords

Choroid plexus; Neuroinflammation; Neurogenesis; Tight junctions.

Resumo alargado

Sendo parte integrante do sistema nervoso central, os plexos coroides (CP) são estruturas ramificadas, altamente vascularizadas, com uma camada de células epiteliais secretoras que projetam numerosas vilosidades nos quatro ventrículos do cérebro. Os CP são constituídos por uma monocamada externa de células epiteliais coroidais (CPEC), cuja membrana apical está em contacto direto com o líquido cefalorraquidiano, enquanto que a membrana basal das CPEC se localiza sobre o estroma. O estroma é rodeado por células dendríticas, fibras de colagénio, fibroblastos e células B e T. Neste conjunto, encontram-se células imunitárias inatas cuja função é apresentar antigénios, moléculas que são capazes de iniciar resposta imune, o que sugere que o CP pode desempenhar um papel ativo na proteção imune do cérebro. Durante muito tempo, pensava-se que o cérebro era uma estrutura "imunologicamente privilegiada", isto é, que o cérebro se encontrasse separado fisicamente do sistema imunitário periférico através da barreira hematoencefálica, não havendo trocas entre o cérebro e o restante organismo. A barreira hematoencefálica em conjunto com a barreira formada pelas CPEC protege o sistema nervoso central contra agentes patogénicos através das junções intercelulares que são compostas por proteínas de integridade de membrana. Estas proteínas permitem ao CP ter capacidade imunitária, uma vez que controlam a permeabilidade celular, impedindo os solutos de água de passar livremente, formando uma fronteira entre os domínios de membrana plasmática apicais e basolaterais, impedindo a passagem de proteínas entre os compartimentos da membrana. Não obstante, a permeabilidade da barreira pode ser influenciada por uma neuroinflamação permanente. A neuroinflamação é caracterizada pela ativação da microglia, *stress* oxidativo e expressão dos principais mediadores inflamatórios sendo um processo ativo de defesa contra vários insultos, lesões traumáticas e metabólicas, infeções e doenças neurodegenerativas tais como a doença de Alzheimer e de Parkinson. Outro "dogma" das neurociências durante muitos anos foi a não existência de neurogénese, isto é, as células do sistema nervoso não se regeneravam. Contudo, estudos recentes afirmam que o CP, quando sujeito a uma agressão, tem capacidade de formar novas células e estas por sua vez são capazes de se diferenciarem. Assim, neste trabalho propusemo-nos a avaliar o efeito de um insulto neuroinflamatório agudo provocado pelo lipopolissacarídeo (LPS), na neurogénese e na neuroinflamação do CP. Mais especificamente, a resposta inflamatória induzida pelo LPS no CP foi avaliada *in vivo, ex vivo* e *in vitro* através da análise de marcadores inflamatórios tais como CD11b, iNOS, expressão de TTR e produção de espécies reativas de oxigénio (ROS) e de óxido nítrico (NO). Avaliámos também o efeito do LPS na neurogénese *in vivo* e *ex vivo* através do estudo da presença de diferentes marcadores: NeuN, CD11b e o GFAP. Por fim, verificámos se o LPS teria algum efeito na integridade da membrana. A resposta inflamatória foi analisada: *in vivo* em CP de ratinhos C57BL/6 injetados com 1,0 mg/kg de LPS e sacrificados 7h depois; explantes de CP

de ratos recém-nascidos e de animais com 21 dias que foram posteriormente incubados durante 48h com 0,1 µg/mL de LPS. A produção de ROS, NO e alterações no teor de proteínas do meio extracelular foi avaliada em CPEC e verificou-se um aumento na produção de ROS e NO e um incremento no teor de proteínas totais do meio extracelular, em CPEC. Foi possível verificar, em explantes de CP, um aumento na expressão de CD11b, um marcador de microglia, e GFAP que é utilizado como um marcador de astrócitos, uma diminuição na expressão de NeuN, um marcador de neurónios maduros e não se verificou alterações na expressão de TTR, a principal proteína decretada pelo CP. Foi realizado *Western blot* para verificar se o CP libertaria TTR para o meio de cultura e se a quantidade desta libertada no meio de cultura das CPEC variava ao longo do tempo, apesar de ter ocorrido libertação de TTR par o meio a sua quantidade manteve-se constante ao longo do tempo. Realizou-se *Western blot* para verificar se havia alterações na secreção de iNOS por parte do CP, tendo sio possível verificar um aumento significativo da enzima nos plexos incubados com LPS comparados com os controlos. O efeito do LPS na integridade do CP como barreira foi analisado através do estudo da expressão das proteínas ocludina, claudina-1, e-caderina e ZO-1 *in vitro* em CPEC, a expressão de ocludina e e-caderina foi também estudada *ex vivo* e *in vivo*. As imagens de imunocitoquimíca referentes às proteínas de integridade de membrana: ocludina, claudina-1, e-caderina e ZO-1, foram adquiridas num microscópio confocal (Zeiss) e a fluorescência emitida foi quantificada. Os resultados revelaram que as CPEC mantiveram a expressão das suas proteínas de integridade de membrana, depois de um insulto com LPS, contudo a expressão da ocludina e da ZO-1 apresentaram uma redução significativa. Por sua vez os resultados *ex vivo* não mostraram nenhuma alteração na expressão de ocludina e e-caderina. Os ensaios *in vivo* confirmaram a expressão de ocludina e e-caderina em CP. Assim, podemos concluir que o CP tem uma resposta ativa à neuroinflamação induzida pelo LPS, o que se comprova pelo aumento das proteínas relacionadas com a resposta imunitária e também com um aumento do stress oxidativo a que as células são sujeitas. Verificou-se também que um insulto neuroinflamatório compromete a diferenciação das células do plexo, havendo decrescimento da neurogénese em todas as experiencias realizadas. Finalmente, outra das conclusões que foi possível conjeturar com este estudo foi, que morfologicamente o CP mantém a integridade da barreira, embora não nos seja possível inferir se esta fica ou não comprometida.

Palavras-chave

Plexo Coroide; Neuroinflamação; Neurogénese; Proteínas de Integridade da Membrana

Table of contents

List of Figures

List of Tables

Abbreviations

Aβ	Beta-amyloid
AD	Alzheimer Disease
AJ	Adherens Junctions
Ara-C	Arabinoside
BBB	Blood Brain Barrier
BCSFB	Blood-Cerebrospinal Fluid Barrier
BSA	Bovine Serum Albumin
CAPS	3-(Cyclohexylamino)-2-hydroxy-1-propanesulfonic acid
CNS	Central Nervous System
CP	Choroid Plexus
CPEC	Choroid Plexus Epithelial Cells
CSF	Cerebrospinal Fluid
DCFH-DA	Dichloro-dihudro-fluorescein-diacetate
DHE	Dihydroethidium
ECF	Enhanced Chemifluorescence
EGF	Epidermal Growth Factor
DMEM	Dulbecco's Modified Eagle Medium
EDTA	Ethylenediaminetetraacetic acid
EGTA	Ethylene glycol tetraacetic acid
FBS	Fetal Bovine Serum
GFAP	Glial Fibrillary Acidic Protein
ICC	Immunocytochemistry
IL	Interleukin
iNOS	inducible NOS
LPS	Lipopolysaccharide
ND	Neurodegenerative Disease
NED	*N*-1- apthylethylenediamine dihydrochloride

NeuN	Neuronal Nuclear Protein
NO	Nitric Oxide
NOS	Oxide Nitric Synthase
PBS	Phosphate Buffered Saline
PBS-T	Phosphate Buffered Saline with Tween
PD	Parkinson Disease
PDVF	Polyvinylidene difluoride
PFA	Paraformaldehyde
PNS	Peripherical Nervous System
ROS	Reactive Oxygen Species
RNS	Reactive Nitrogen Species
SDS	Sodium Dodecyl Sulfate
SEM	Standard Error of the Mean
TBS	Tris Buffered Saline
TBS-T	Tris Buffered Saline with Tween
TNF	Tumor Necrosis Factor
TJ	Tight Junctions
TLR	Toll Like receptor
TTR	Transthyretin
WB	Western Blot
WM	Whole Mount
ZO	Zonula Occludens

Chapter 1: Introduction

1. Introduction

1.1 Nervous System

The human nervous system is highly integrated and can be divided in two parts: the central nervous system (CNS) and the peripheral nervous system (PNS). The CNS includes the brain and spinal cord and it is the integrating and commanding centre of the nervous system. It interprets sensory input and dictates motor responses based in memory (past experience), reflexes and current conditions. The PNS, the part of the nervous system outside the CNS, consists mainly of nerves that extend from the brain and spinal cord. It serves as communication thread that links all parts of the body to the CNS(1). CNS consists of neurons and glial cells. Among glial cells, astrocytes constitute nearly 40% of the total CNS cell population in the adult human brain while microglia cells are derived from myeloid cells and comprise approximately 12% of cells in the brain (2).

Astrocytes guide the development and migration of neurons during brain development, production of growth factors, maintenance of the integrity of the blood-brain barrier (BBB), and participate in the immune and repair responses to diseases and brain injury (3, 4). Microglial cells represent resident brain macrophages and can be transformed into activated immunocompetent antigen-presenting cells during the pathological process.

The cell-cell interactions between glial cells and neurons may be important in the regulation of brain inflammation and neurodegeneration (2).

1.2 Choroid Plexus

The choroid plexus (CP) arises from the ependymal lining of the brain ventricles and protrude into the ventricles of the brain (5).

In the brain there are four CP, with tissues in each lateral, third and fourth ventricles (6). The lateral plexus are thin leaf-like undulated structures arising from the inner ventricular surface, the third plexus protrudes from the roof of the third ventricle, and the fourth plexus is formed caudally and ventrally to the cerebellum: the CP in the third and forth ventricles are branched villi that protrude into the ventricle (6).

CP tissues comprise a continuous monolayer of cuboidal (7) and columnar epithelial cells localized over connective tissues, underneath the basement membrane (8).

These ciliated epithelial cells are characterized by numerous mitochondria spread throughout the cytoplasm, a central nucleus, and an abundant Golgi apparatus located laterally and toward the ventricular lumen (8). Depending on the physiological or pathological conditions, the epithelial cells lie on an epithelial basement membrane surrounding a thin stroma with numerous collagen fibbers, dendritic cells, macrophages, fibroblasts, B and T cells, and large capillaries with a fenestrated endothelium (9, 10). Some of these cells are innate immune cells whose main function is antigen presentation which suggests that the CP may play an active role in immunological brain protection (10, 11). CP are richly innervated, receiving adrenergic, cholinergic, peptidergic and serotoninergic fibers. The distribution of nervous fibers varies widely according to species (11). CP cells are connected by junctional complexes at the luminal membrane, consisting of tight junctions (TJ), adherens junctions (AJ) and desmosomes (Figure 1).

Beneath the epithelial basement membrane is a network of fenestrated capillaries that are surrounded by connective tissue composed by fibroblasts and immune cells. The fenestration of capillaries are sealed with thin diaphragms, which permit ions, water and small molecules, as nutrients or vitamins, to pass without difficulty into the interstitial fluid of each plexus(8).

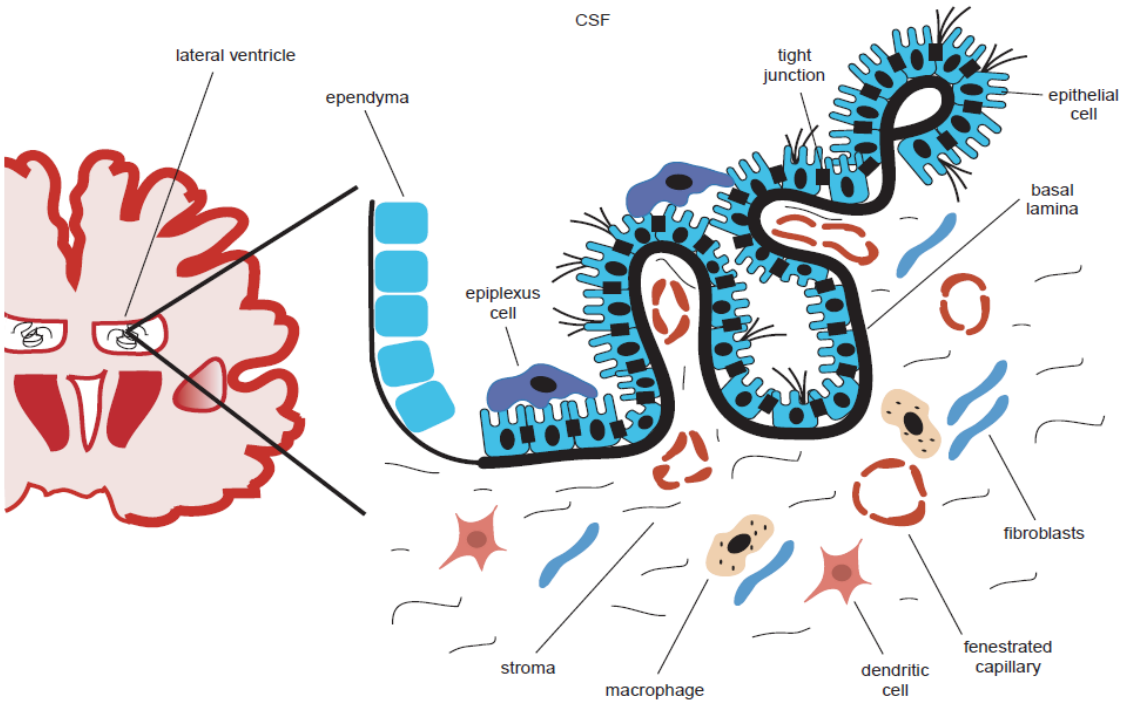

Figure 1: Schematic illustration of choroid plexus as it resides within the lateral ventricle (left) and as defined by its morphological appearance (right). CSF – Cerebrospinal fluid. (Adapted from Emerich et. al., 2004 (12)).

1.2.1 Choroid plexus functions

Due to its many functions, relying primarily in the unique structure of the epithelial cells, CP is considered a multipurpose organ (7). The best known function is cerebrospinal fluid (CSF) formation, which not only regulates homeostasis in the CNS, providing buoyancy for the brain and spinal cord, but also participates in neural stem cell renewal, neuroprotection, sleep/awake cycles and in several neurological disorders, as Alzheimer Disease (AD) and Parkinson Disease (PD) (13). In humans, CSF volume is 0.37 mL/min, almost 500 mL/day (10). CSF is produced mainly by active secretion, with water entering the CSF from the blood along an osmotic gradient or by specific water channels such as aquaporins. The epithelial CP cells secrete CSF by moving sodium, chloride and bicarbonate (the bicarbonate can also be synthesized in the epithelial cells using the carbonic anhydrase enzyme) from the blood to the ventricles to create the osmotic gradient that drives the secretion of H_2O. The CSF is a clear fluid, with few cells and little protein, and has a lower pH and concentration of glucose, potassium, calcium, bicarbonate and amino acids compared with blood plasma. On the other hand the sodium, chloride and magnesium content is greater in CSF than in plasma (10). CP participates not only in the synthesis, secretion and regulation of several biologically active compounds of the CSF but also in the maintenance of brain metal bioavailability and in the surveillance of toxic compounds in the CSF, thereby protecting the brain against neurotoxic insults (14).

CP is ideally located to distribute molecules both locally and globally to the brain due to its secretor capacity into the CSF. The CP possesses several specific transport systems, containing an array of receptors and also serves as a source of biologically active products. The CP epithelium is not only a target but also a source of neuropeptides, growth factors and cytokines for the CSF (15).

1.2.2 Brain barriers: Endothelial Versus Epithelial Cells of CP

The BBB and the blood-CSF barrier (BCSFB) protect the CNS from the changeable milieu of the blood stream to establish CNS homeostasis, which is a requirement for proper neuronal function. Whereas the BBB is located at the level of highly specialized endothelial cells within CNS microvessels, the BCSFB is formed by the epithelial cells of the CP (16).

The intercellular junctions of the BBB endothelial cells and of the CP epithelial cells are composed by TJ and AJ. The TJ are constituted by: claudins, occudins and juctional adhesions molecules and the AJ are constituted by cadherins (Figure 2).

1.3.1 Tight Junctions and Adherens junctions

Tight junctions form channels that allow permeation between cells, resulting in epithelial surfaces of different tightness (17). A TJ is an intercellular adhesion complex ensuring close contact between adjacent cells and are found in the apical region of the cell (18). TJ control the paracellular permeability across lateral intercellular spaces preventing solutes and water from passing freely through the paracellular pathway, and form a boundary between the apical and basolateral plasma membrane domains by preventing diffusion of proteins between the membrane compartments (18, 19). TJ are important components of numerous signaling pathways controlling gene expression, cell differentiation and proliferation.

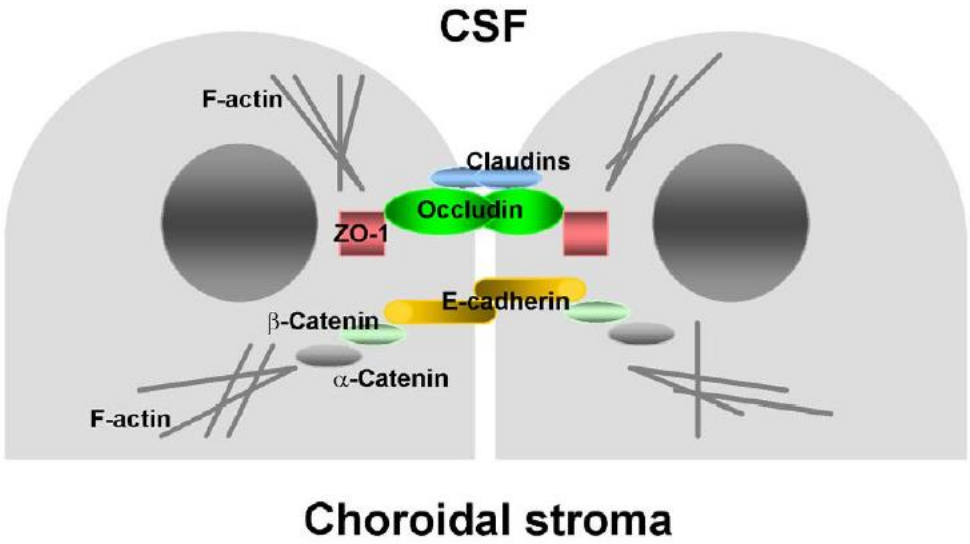

Figure 2: Schematic representation of tight junctions and adherens junctions complexes in choroidal epithelial cells (adapted from Szmydynge-Chodobska et.al., 2007 (20)).

Occludin was the first TJ integral membrane protein identified. This ~64 kDa protein specifically located at TJs of epithelial and endothelial cells is incorporated into the network of TJ strands. Occludin consists of four transmembrane domains, two extracellular domains, and three cytoplasmatic domains (21), forming a homophillic dimmer (21). Occludin interacts with the actin cytoskeleton and several intracellular proteins. Its over expression increases electrical resistance, implying a pro-barrier phenotype and increases permeability to small molecule tracers (22). Occludin, as well as claudin-1, claudin-2, and claudin-11, has been reported to be expressed in choroidal epithelium (13).

Similar to occludin, claudins have four transmembrane domains, two extracellular loops and a short carboxyl intracellular tail (22). The claudin's family consists of at least 24 members with molecular weight from 20 to 27 kDa. Claudins' extracellular loops form the back none of TJ by forming dimmers and binding homotypically to other claudin molecules in adjacent endothelial cells.

Zonula Occludens (ZO) proteins are classified as members of the membrane associated guanylate kinase family. These proteins are thought to have both structural and signaling roles, and are characteristically defined by three protein-protein interaction modules. The way by which ZO proteins interact with the membrane proteins appears to be specific to each type of membrane protein (22).

E-cadherins comprise a member family of calcium - dependent adhesion molecules. The intracellular domain of E-cadherin binds to ß-catenin, and to α-catenin, which in turn interacts with actin, and this catenin-mediated anchorage of E-cadherin to the actin cytoskeleton is required for strong cell-cell adhesion. E-cadherin, as a mature protein, have molecular weight between 80 and 120 kDa, but it is approximately 135 kDa if we considered the molecular weight of the precursor. E-cadherin is a protein that functions to mediate cell-cell binding critical to the maintenance of tissue structure and morphogenesis.

Occludin and the members of the family of claudin proteins are the major constituents of TJ, they are connected to the actin filaments through cytoplasmic adaptor proteins, ZO-1, members of the membrane-associated guanylate kinase family of proteins (23). Interestingly, ZO-1 not only binds to occludin and claudins, but is also able to interact with α-catenin (24). However, in epithelial cells bearing well-developed TJs, ZO-1 does not co-localize with AJ (25).

The permeability of BBB could be altered by the chronic inflammatory pain (26). The inflammatory process disrupts the integrity of BBB and is associated with decreasing of the expression of occludin, promoted by the disruption of occludin oligomeric assemblies (21). Some recent studies support that the expression of claudin-1 and E-cadherin in animals with or without inflammation showed similar results, meaning that the expression is not influenced by neuroinflammation (19, 26). Comparing the immunoreactivities for ZO-1 in the CP between healthy mice and infected mice, it was observed differences in immunoreactivity for the TJ proteins investigated. Importantly, even under inflammatory conditions all TJ associated proteins remained expressed properly (24). In conclusion, brain barriers are able to mount, at least, an initial response to peripheral inflammation, either in reaction to infiltration of inflammatory mediators to the CNS, or due to the effects of infiltration of activated peripheral immune cells, and this vascular inflammatory response may in itself contribute significantly to neuroinflammatory disease (19).

1.3 Neuroinflammation

Being physically separated from the peripheral immune system, the CNS is conventionally recognized as being “immunologically privileged”. Immune privilege in the CNS is partially dependent on the BBB, which is intended to limit the entry of solutes and ions into the CNS.

The precise mechanisms through which peripheral inflammation stimuli trigger brain are poorly understood (27).

Neuroinflammation is characterized by the activation of microglia and expression of major inflammatory mediators without typical features of peripheral inflammation such as edema and neutrophil infiltration. Neuroinflammation is an active defensive mechanism against several insults, metabolic and traumatic injuries, infections and neurodegenerative disease (ND) (22). Moreover, it causes cognitive impairment, even if is acutely stimulated by immunostimulatory component such as lipopolysaccharide (LPS).

Bacterial molecules such as LPS, a component of the external cell membrane of gram negative bacteria (28), have the capacity to activate different groups of cells in CNS: microglia, astrocytes and mast cells (29).

Activation of microglia is a characteristic found on the most CNS autoimmune disorders, which represent the main effector cells of the immune system in the CNS, and its chronic state contributes to progression of ND. Most of the relevant mechanistic studies that are related to neuroinflammation have been carried out in the context of AD and PD. However, a role for neuroinflammation in the pathogenesis of other ND is also emerging. Studies suggest a role for innate immune activation in the pathogenesis of frontotemporal dementia, amyotrophic lateral sclerosis and Huntington's disease (30). The role of microglia in demyelingting disease is controversial and both protective and degenerative functions have been proposed (29, 31). Under acute injurious conditions microglial activation is among the first immune-related events at the lesion site (Figure 3), yet it seems that microglia either cannot acquire a resolving-phenotype, or fail to be skewed to this phenotype in a time-dependent manner.

Under physiological conditions, microglia stay as a quiescent population, but upon exposure to LPS, microglia are activated and produce pro-inflammatory mediators such as cytokines, chemokines, prostanoids, reactive oxygen species (ROS) and nitric oxide (NO). Microglia are the primary cellular source of pro-inflammatory cytokines, including tumor necrosis factor-α (TNF-α) and interleukin (IL)-1ß, and is characterized by an increased proliferation and morphological changes (32).
Mast cells can be found within the brain and their functions include the attractant and activation of other immune cells by secreting pro-inflammatory cytokines, and chemoattractants (33). Finally, astrocytes also contribute to the immune response by liberating both pro- and anti-inflammatory cytokines, chemokines and complement components (4, 34).

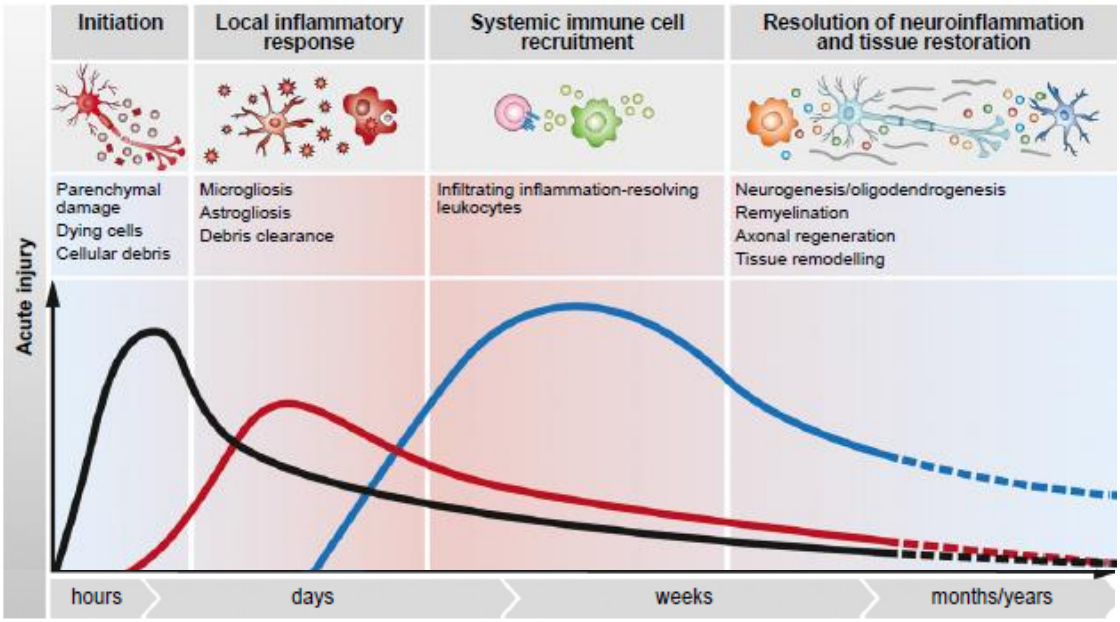

Figure 3: Local immune cell response to acute and chronic Central Nervous System. (Adapted from Schwartz et. al., 2014 (35))

1.3.1 Indicators of neuroinflammation

One indicator of neuroinflammation is oxidative stress which occurs when the homeostatic processes fail and free radical generation is much beyond the capacity of the body's defenses, thus promoting cellular injury and tissue damage (36) .
ROS formation occurs continuously in the cells as a consequence of both enzymatic and non-enzymatic reactions (36). They participate in several physiological mechanisms such as cellular signaling, gene expression and pathogen elimination (37). However, at high levels, ROS can cause irreversible and detrimental cellular damage.

Closely related to ROS are the reactive nitrogen species (RNS). NO is produced by constitutive Nitric Oxide Synthase (NOS) during vasodilating processes or during transmission of nerve impulses. In the presence of insults, NO is produced by catalytic action of inducible NOS (iNOS) and is present at higher concentrations (38, 39). NO can cause damage to proteins, lipids and DNA either directly or after reaction with superoxide, leading to the formation of very reactive peroxynitrite anion. In a healthy brain, the level of iNOS is undetectable (2). In CNS, upregulation of iNOS in various cells types, including astrocytes and microglia, is proposed to be the leading source of NO production during neuroinflammation (2).

Neurodegenerative diseases are characterized by a "redox state" imbalance (representing a disparity between formation of ROS and RNS and elimination by various reducing or antioxidant systems) and chronic inflammation, a major cause of cell damage and death (2).

1.4 The choroid plexus in neuroinflammation

The CP can be seen as the first line of defense in the brain against harmful stimulus, whether they are molecules, cells or pathogens. The presence of the CP TJ prevents the passage of several toxic compounds into the CSF. The CP is also involved in the interaction between the peripheral immune system and the brain. In their studies, Engelhard et al. demonstrated that CP epithelial cells and CP stroma allow the communication between a peripheral inflammatory stimulus and the initiation and development of an innate and adaptive response in the brain (22). Following systemic activation of the immune system by the administration of LPS there is a rapid and transient induction, in the CP, of immune-modulators such as Il-1ß and TNF-α (31). Activation of the CP may certainly spread throughout the brain indicating that the CP transmits information between the immune system and the brain through the BCSFB.

Structurally, the BCSFB lacks endothelial TJ or astrocytes-glial limiting membrane. This relative structural permissiveness for immune cell trafficking, and the fact that the cellular ventricular composition of the take to suggestion that T cells enter the CSF, in a regulated manner, via the CP. Unlike the BBB, the CP constitutively expresses adhesion molecules and chemokines, which support transepithelial leukocyte trafficking (40). Accessory molecules, important to leukocytes, are found expressed at low levels in CP epithelial cells but can also be up-regulated during inflammation.

Transthyretin (TTR) is a major protein synthesized by the epithelial cells of the CP by CSF, where its synthesis represents approximately 20% of the total protein synthesis (41). TTR is also synthesized by the liver to the peripheral circulation (42). Its main function is the transport of thyroid hormones and the indirect transport of retinol via its binding to plasma retinol-binding protein (43) that are essential for normal brain development (44). Some studies reported that TTR acts as an endogenous detoxifier of protein oligomers through the inhibition of amyloid fibril formation with potential neuroprotective effects in AD (41, 45).

1.5 Neurodegenerative diseases

Neurodegeneration, the progressive dysfunction and loss of neurons in the CNS, is the major cause of cognitive and motor dysfunction (32). Neuronal degeneration is well-known in AD and PD.

1.5.1 Alzheimer Disease

Alzheimer disease accounts for up to 70% of all diagnosed cases of dementia, an age-related condition which affects approximately 36 million people worldwide (46). AD is a progressive and irreversible ND associated with cognitive decline (47, 48), with the presence of senile plaques, neurofibrillary tangles, persistent neuronal loss deterioration (48) and proliferation of reactive astrocytes in the cortex, hippocampus, amygdala and associated areas of frontal,

temporal, pariental and occipital cortex. The observed symptoms are related to pariental dysfunction and difficulty in word-finding commonly develop fairly early in the course of the disease, and deficits in attention, work, memory and other aspects of executive functions (49).

Studies performed in AD field strongly support the hypothesis that amyloid beta (Aβ) deposition in the brain is the primary event in AD progression (50). Aβ protein and oxidative stress are believed to play central roles in AD development preceding Aβ pathology and neurofibrillary tangles (51).

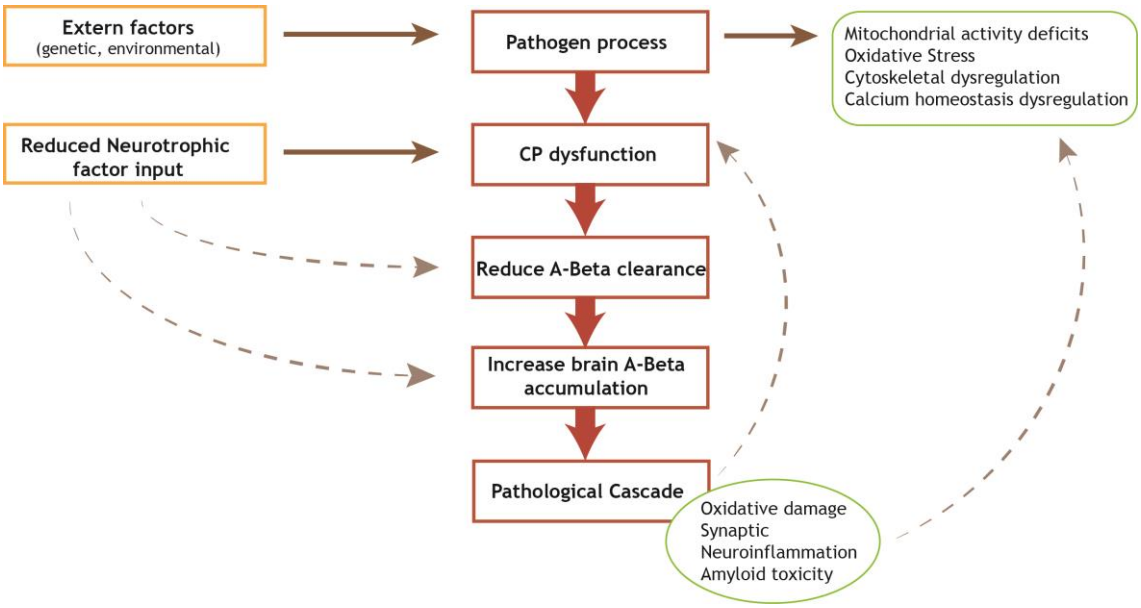

Figure 2: Proposed sequence of pathological processes involved in Alzheimer's disease. Various pathogenic processes contribute to the dysfunction of the choroid plexus which results in impaired Aß processing. This and the resultant accumulation of Aß can in turn feed back to enhance the pathogenic processes. CP-Choroid Plexus; Aß-amyloid beta. (Adapted from (52))

1.5.2 Parkinson Disease

Parkinson disease is the most common neurodegenerative movement disorder, and the second most common ND, affecting nearly 4 million people worldwide. It is characterized by progressive hypokinesia, slowness of movement, rigidity, development of a resting tremor, and loss of postural reflex (53).

The hallmarks of neuroinflammation, in PD, are the presence of activated microglia and reactive astrocytes in the parenchyma (neurons, astrocytes, and endothelial cells) of the CNS, direct participation of the adaptive immune system, increased production of cytokines, chemokines, prostaglandins, a cascade of complement proteins, ROS and RNS, which in some cases can result in disruption of the BBB (54). The extent to which neuroinflammation and peripheral immune responses contribute towards the development of PD or modify its course is not exactly known (54, 55).

1.6 Neurogenesis

Before the 1990s, it was consensual that neurons in the adult brain were not regenerated. Consequently, it was thought that if neurons died during the adult life for any reason (e.g., oxidative stress, stroke, ND, head trauma, normal aging), they would never be replaced (56). The first evidence that neurogenesis occurs in the adult rodent brain was described by Altman and Das in 1965 (57), where they report that new neurons are continuous and spontaneously born in only two specific brain regions: the subgranular zone of the hippocampus, with cells migrating to the granule layer of the dentate gyrus and the subventricular zone with cells migrating to the olfactory bulb (56, 58). The hippocampus is critical to learning and memory as well as mood regulation, and adult neurogenesis necessary for normal function (58). Notably, the hippocampus is also particularly vulnerable in AD.

Due to the longstanding dogma that postnatal neurogenesis is non-existent in mammals, it took many years before the Altman and Das discovery was broadly accepted.
Multi-potent stem cells divide asymmetrically producing one daughter progenitor cell and one stem cell. The progenitor cell can then divide asymmetrically producing daughter cells that differentiate into either astrocytes or neurons and one progenitor cell retains the capacity to divide multiple times (56).

1.7 Relationship between neurogenesis and neuroinflammation

The effect of neuroinflammation in neurogenesis can have negative and positive consequences, which can result in development or inhibition of the process. The effect relies principally on how inflammatory cells are activated and for how long the inflammation occurs (59). We can distinguish two types of inflammation: acute and chronic inflammation. Acute inflammation comprises the immediate and early response to an injurious agent and is basically a defensive response that paves the way for repair of the damaged site being typically short-lived and unlikely to be detrimental to long-term neuronal survival. The chronic response occurs when the harmful stimulus persists over time, and contrary to the acute form, it is a long-standing and often self-perpetuating neuroinflammatory response which, in the end, results in detrimental consequences for neurons. In chronic inflammation, as AD, neuroinflammation has also been shown to induce a blockade in neurogenesis. The direct mechanism as how neuroinflammation is able to induce a disruption to neurogenesis has not yet to be fully elucidated. Some studies performed by Monje et al. revealed that peripheral administration of LPS, inducing an increase in central pro-inflammatory cytokine production, was sufficient to induce a 35% decrease in hippocampal neurogenesis (60). This disruption of neurogenesis by LPS was also shown to be able to induce spatial learning and memory deficits task, symptoms observed in AD. However, some aspects of the neuroinflammatory response result in beneficial outcomes for CNS. Among these benefits,

neuroprotection phenomena, the maintenance of neurogenesis as a mechanism of brain repair, the mobilization of neural precursors for repair, remyelinization, and even axonal regeneration are included. The final result depends largely on how microglia, macrophages, and/or astrocytes are activated and the duration of the inflammation (59).

Chapter 2: Aim

2. Aim

The main goal of this work was to evaluate the effect of an acute neuroinflammatory insult to the neurogenic potential, protein synthesis and barrier function of the CP. More specifically:

i) the inflammatory response induced by LPS in CP will be assessed *in vivo*, *ex vivo* and *in vitro* through analysis of inflammatory markers such as CD11b, iNOS, changes in TTR expression, and production of ROS and NO.

ii) the effect of LPS in CP neurogenesis *in vivo* and *ex vivo* will be analysed by studying the presence of the mature neuron marker, NeuN, the microgial marker ,CD11b and the astrocyte marker, Glial Fibrillary Acidic Protein (GFAP) in CP.

iii) the effect of LPS in CP integrity as a barrier will be analysed by assessing its effects on TJ proteins *in vitro*.

Chapter 3: Materials and Methods

3. Materials and Methods

3.1 Animals

Animals were handled in compliance with the National Institutes of Health guidelines and the European Union rules for the care and handling of laboratory animals (Directive 2010/63/EU). Animals' experiments were also performed according to the Portuguese law for animal well being and the protocol approved by the Committee on the Ethics of Animal Experiments of the Health Science Research Centre of the University of Beira Interior (DGV/2013). Beyond that, all efforts were made to minimize animal suffering.

Tissue sampling for *in vitro* and *ex vivo* experiments and from *in vivo* experiments was carried out in animals decapitated under anesthesia with intraperitoneal injection of ketamine hydrochloride (150 mg/kg) plus medetomidine (0.3 mg/kg) and transcardially perfused with cold saline. The brain was removed and CP from the lateral ventricles kept for further analysis.

3.1.1 Primary Cultures of rat Choroid Plexus epithelial cells

The method used for the establishment of primary culture of CEPC has been previously described by Martinho *et al*. (43). Briefly, postnatal rats, with 3-5 days, were sacrificed and CP were dissected under conventional light microscopy from lateral ventricles. CP was rinsed twice in Phosphate Buffered Saline (PBS) without calcium and magnesium and digested with 0.2% pronase (Fluka) in PBS at 37˚C for five minutes. Pre-digested tissues were recovered by sedimentation in Dulbecco's Modified Eagle Medium – high glucose (DMEM, Sigma) with 10% fetal bovine serum (FBS, Biochrom AG) and 100 units/mL of penicillin/streptomycin (Sigma). Cells were pelleted by centrifugation and were resuspended in DMEM supplemented with 100 units/mL antibiotics, 10% FBS, 10 ng/mL, epidermal growth factor (EGF, Sigma), 5 µg/mL insulin (Sigma), 20 µM cytosine arabinoside (Ara-C, Sigma) and were seeded in 12 wells with a 15 mm lamella inside for immunocytochemistry (ICC) or in a 96 well plate (VWR) for ROS, NO and extracellular protein studies. Cells were grown in a humidified incubator at 37ºC with 5% CO_2. The growth medium was changed 1 day after the initial seeding and every 2 days thereafter until they were differentiated.

3.2 Effect of LPS in CP

3.2.1 Effects of LPS in Choroid Plexus Epithelial Cells.

Newborn *Wistar Han* rats, between 3 and 5 days, were sacrificed, and CP from lateral ventricles were removed, for CPEC isolation.

Once differentiated CPEC were serum starved for four hours, and were incubated with culture medium containing 0.1 µg/mL of LPS (Sigma). Cells were recovered for further analysis after 1, 2, 4, 6, 8, 12, 18 or 24 hours of incubation with LPS, and analysed for ROS production, NO production, and quantification of extracellular medium protein was performed (Figure 4). TTR and iNOS expression were also analyzed in cells and in the extracellular medium by Western blot (WB), for different times of incubation with 0.1 µg/mL of LPS (Figure 4).

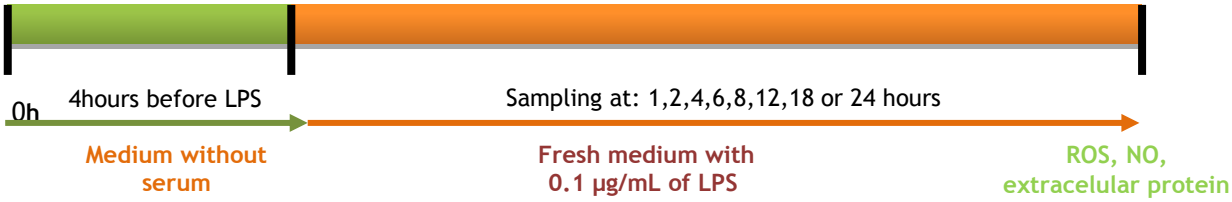

Figure 4: Schematic representation of the procedure to study the production of ROS, NO and protein extracellular in the culture medium, *in vitro*. CPEC were incubated with culture medium with 0.1 µg/mL of LPS for different hours 1, 2, 4, 6, 8, 12, 18 and 24 hours, after. LPS- lipopolysaccharide; ROS- Reactive Oxygen Species, NO- Nitric Oxide

Impairments in CPEC barrier proteins (occludin, claudin-1, ZO-1 and E-cadherin) were evaluated by ICC. For this propose CPEC were serum starved 4 hours and incubated with 0.1 µg/mL of LPS during 24 hours (Figure 5). All experiments were performed independently by three times.

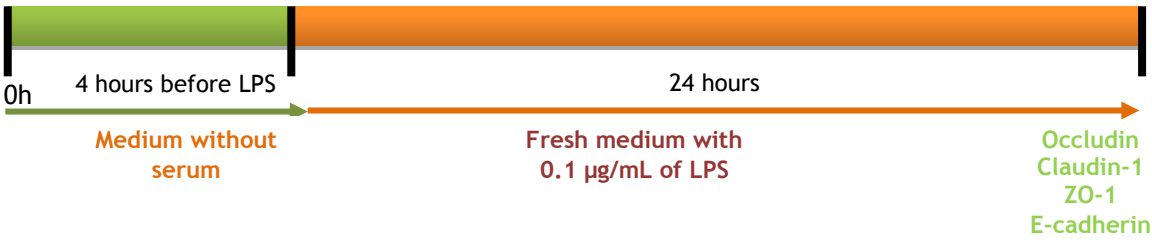

Figure 5: Schematic representation of the procedure performed to study the effects of the LPS insult in tight junctions by immunocytochemistry. CPEC were incubated with 0.1 µg/mL of LPS during 24 hours after being serum starved for 4 hours. LPS- lipopolysaccharide ; ZO- Zonula Occludens.

3.2.2 Effects of LPS in neurogenesis and inflammatory markers in Choroid Plexus explants

To study the effect of LPS in neurogenesis of CP explants, newborn *Wistar Han* rats (P3-P5) and 21 days rats were used, CP from lateral ventricles were extracted and placed directly in serum free culture medium (DMEM) during 4 hours followed by 48 hours incubation with LPS 0.1 μg/mL at 37ºC in an atmosphere containing 5% of CO_2. After incubation, CP explants were analysed by whole mount (WM), using the following markers: NeuN, GFAP, CD11b and TTR. This experiment was repeated for protein extraction followed by WB (iNOS, TTR, E-cadherin and occludin), and for analysis of ROS production (Figure 6).

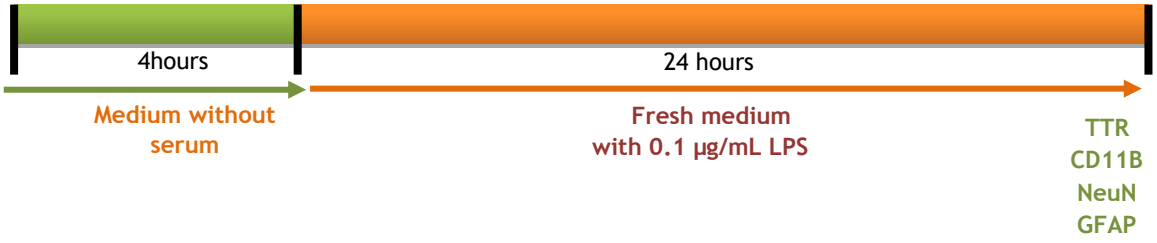

Figure 6: Schematic representation of the procedure performed to study neurogenesis in CP explants upon an inflammatory insult with 0.1 μg/mL of LPS *ex vivo*. LPS- lipopolysaccharide, TTR- Transthyretin, NeuN- Neuronal Nuclear Protein, GFAP- Glial Fibrillary Acidic Protein.

3.2.3 Inflammatory response of CP to a LPS insult, *in vivo*

C57BL/6 mice with 1, 3 and 9 months old were randomly divided into two groups at the beginning of the experience: the control group and the experimental group (9 animals in each group). In the experimental group, a single intraperitoneal dose of LPS (1.0 mg/kg) dissolved in NaCl (0.9%, pH 4.5 -7.0) was administered. Control group received an intraperitoneal dose of NaCl (0.9%, pH 4.5 -7.0). To reduce the stress-induced changes in the hypothalamus and pituitary axis, animals were handled for one week before injections (Figure 7). CP were collected 7 hours after LPS injection directly to protein extraction buffer. Protein extracts from these CP were used to compare the expression of iNOS, TTR, E-cadherin and occludin, by WB upon an inflammatory acute insult during aging.

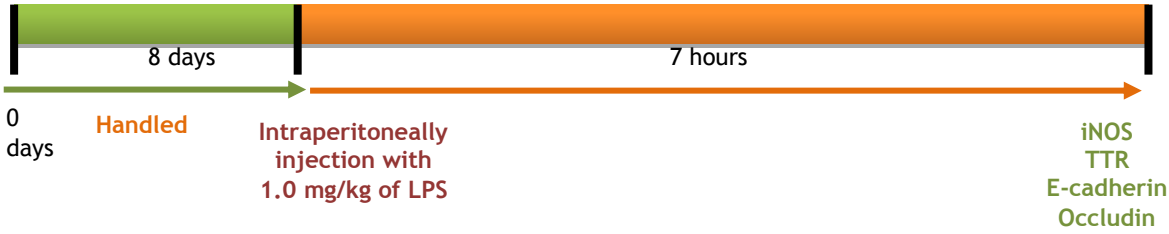

Figure 7: Schematic representation of the experimental layout to analyze the response of CP to 1.0 mg/kg of LPS inject *in vivo*. LPS- lipopolysaccharide, iNOS- inducible nitric oxid synthase, TTR- transthyretin.

3.2.4 Neurogenesis in CP *in vivo* in response to a LPS insult

C57BL/6 mice, of different ages, 1 and 3 months old, were intraperitoneal injected with LPS (1.0 mg/kg) or with vehicle (0.9% NaCl, pH 4.5- 7.0). Mice were randomly divided into two groups at the beginning of the experience, with 9 animals each. To reduce the stress-induced changes in the hypothalamus and pituitary axis, animals were handled for one week before injections. CP were collected 28 days after LPS injection directly to 4% paraformaldehyde (PFA) and used for detecting Neuronal Nuclear Protein (NeuN), CD11b, GFAP and TTR by WM (Figure 8).

Figure 8: Schematic representation of the procedure performed to assess neurogenesis upon LPS insult *in vivo*. LPS- lipopolysaccharide, TTR- Transthyretin, NeuN- Neuronal Nuclear Protein, GFAP- Glial Fibrillary Acidic Protein.

3.3 Assessment of ROS production, inflammatory response and neurogenesis markers

3.3.1.1 ROS production in CPEC

ROS production was determined with dihydroethidium (DHE, Life technologies). In this assay, blue fluorescent DHE is dehydrogenated by superoxide to form red fluorescent ethidium bromide (61). At the end of the experiments described in 3.6.1, cells were incubated for 4 hours with DHE 5 μM. Finally, fluorescence was measured at 620 nm in a microplate reader spectrofluorometer, Anthos 2020 (62).

3.3.1.2 ROS production in CP explants

Intracellular ROS was measured in CP explants by dichloro-dihudro-fluorescein-diacetate (DCFH-DA, Sigma) oxidation. DCFH-DA enters cells passively and is deacetylated by esterase to form non-fluorescent product DCFH, and DCFH reacts finally with ROS to form the fluorescent product, DCF (61, 63).

CP were incubated with 10 μM DCFH-DA, dissolved in DMEM, for 20 minutes at 37ºC, in dark. Unincorporated DCFH-DA was removed by washing the tissues twice with PBS. To stain DNA, CP were incubated with Hoechst 33342 (1:1000) 20 minutes at 37ºC and after a final wash with PBS fluorescence was quantified, immediately, at wavelengths of 488 nm for excitation and 510 nm for emission under a LSM710 confocal laser scanning microscope (Carl Zeiss, Jena, Germany).

3.3.2 Nitric oxide production in CPEC

The culture medium of CPEC from experiment 3.3.2 (50 µL) was collected to estimate NO concentration by measuring the amounts of nitrite secreted by CPEC into the culture medium, using a colorimetric reaction using the Griess reagent (Promega). This assay relies on a diazotization reaction that was originally described by Griess in 1879, and is based on the chemical reaction which uses sulfanilamide and NED (*N*-1-apthylethylenediamine dihydrochloride) under acidic conditions (62). The culture supernatants were mixed with an equal amount of the Griess reagent in a 96 well plates (Corning). The absorbance of the mixture was read at 542 nm using a microplate reader, Spectra MAX Gemini EM, Molecular Devices.

3.3.3 Protein extraction from CP

CP collected from animals in the experiments described in sections 3.2.2 and 3.2.3, were homogenized in protein extraction buffer (Tris-HCl 25mM Tris-HCl 25 mM pH 7.4, Ethylenediaminetetraacetic acid (EDTA) 2.5 mM, Ethylene glycol tetraacetic acid (EGTA) 2.5 mM, Triton X-100 2%, PMSF 1.0 mM and 10 µL/mL, Complete EDTA Free protease inhibitor cocktail (Roche) 10 µL/mL). After a centrifugation at 10,000xG for 10 minutes at 4ºC supernatants were collected and the total protein quantified.

Protein measurement was performed by the Bradford Method with the Bio-Rad protein assay reagent (Bio-Rad) following the manufacturer's instructions. This method is a colorimetric assay which involves the addition of an acidic dye to protein solution, the absorbance maximum for an acidic solution of Coomassie® Brilliant Blue G-250 dye shifts from 465 nm to 595 nm when binding to protein occurs.

A set of standards (0-10 µg/mL) was prepared from a stock solution of Bovine Serum Albumin (BSA). The Bradford values obtained for the standard were then used to construct a standard curve and used to determine the concentration of our samples. Measurements were performed in 96 well plates after 15 minutes incubation at room temperature. Quantification of the proteins was performed with a microplate reader, Anthos 2020, at 595 nm. After quantification protein extracts were stored at -80ºC until use.

3.3.4 SDS-PAGE and Immunoblot

WB is a method to detect proteins in a given sample of tissue or cells homogenate or extract. It gives information about the size of the proteins (by comparison with a size marker or ladder in kDa), and also gives information on the relative protein expression.

25 µL of samples from section 3.2.1 and 30 µg of each sample obtained from experience described in section 3.2.2 and 3.2.3 was denaturated at 100ºC for 10 min. Then denaturated samples were loaded in a 4.7% stacking gel (4.7% of acrylamide (Applichem), 1.25 M Tris-HCl (pH 6.8, Biorad), 10% Sodium Dodecyl Sulfate (SDS), 7.2 mL H_2O) followed by a 12% SDS-polyacrylamide gel (12% of acrylamide, 1.875 M Tris-HCL, 0.2% SDS, 5.95 mL H_2O) with the NZY Colour Protein Marker II, molecular weight marker (NZYTech) as a reference. A voltage of

120 V was applied and after separation in an electrophoresis system from Cleaver, proteins were blotted onto a polyvinylidene difluoride (PDVF) membrane (GE Healthcare). Therefore, a wet transfer was performed. For that PDVF membrane was previously activated in 100% methanol and equilibrated in transfer buffer (10 mM 3-(Cyclohexylamino)-2-hydroxy-1-propanesulfonic acid (CAPS) from Bio-Rad, 10% methanol).

To blot the samples into the PDVF membrane, a Bio-Rad system was used. The transfer sandwich consisted in a fiber pad, one filter paper soaked with transfer buffer the gel and the PDVF membrane. Two layers of wet filter paper and finally one fiber pad. Once completed the transfer sandwich was transferred to the gel holder cassette and put in the support. Blotting was performed for 30 minutes to TTR (14 kDa) and 1:30h to iNOS (130 kDa), E-cadherin (135 kDa), occludin (60-82 kDa), with a voltage of 750 mA. The difference in blotting times is due to the protein size.

Once protein transfer finished, the membrane was washed twice with Tris Buffered Saline (TBS) for 5 min at room temperature. Afterwards, membrane was blocked with 0.5% non-fat dry milk (Paturages) dissolved in TBS 0.1% Tween (TBS-T). After rinsed with TBS-T, the primary antibody against TTR, iNOS, E-cadherin and occludin was applied overnight at 4°C in the appropriate dilution in TBS-T (see tables 1 and 2). The membrane was washed three times with TBS-T 0.1% for 15 min at room temperature and incubated for 1 hour at room temperature with the correspondent secondary antibody alkaline phosphatase linked dissolved in TBS-T.

Protein detection was done after three washing steps of 15 minutes with TBS-T, immunoreactive bands were detected using the Enhanced Chemifluorescence (ECF) subtract, fluorescent substrate for alkaline phosphatase-based detection of protein blots (GE Healthcare) and images were acquired with the Molecular Imager FX Pro Plus MultiImager system (Bio-Rad). Proteins expression was quantified by densitometric analysis using the QuantityOne software from Bio-Rad. The β-actin protein was chosen for normalize the data of protein expression.

3.3.5 Immunocytochemistry

Immunocytochemistry is a technique used to verify the presence of a specific protein or antigen in cells, using specific antibodies. ICC is a valuable tool to study the presence and sub-cellular location of proteins.

Cells were fixed with 4% PFA in 0.1 M PBS, pH 7.4, for 10 minutes, at room temperature. Subsequently cells were block with 20% FBS in PBS for 60 minutes followed by the primary diluted antibody incubation in 1% FBS in PBS, overnight at 4ºC (Table 1). The primary antibody was removed and cells were washed with PBS. Cells were incubated with the secondary antibody for one hour at room temperature in the dark (Table 2). For counter staining, cells were incubated with Hoechst 33342 (1:1000, Invitrogen) in PBS, for 10 minutes at room temperature in the dark. Afterward preparations were covered with a coverslip with a drop of

mounting medium Entellan (Merck). Slides were stored in the dark at -20ºC and analysed under a LSM710 confocal laser scanning microscope (Carl Zeiss, Jena, Germany).

3.3.6 Whole Mount technique

Whole Mount is used to determine the cellular location and distribution of a given protein in a tissue by the use of specific antibodies.

CP were fixed with 4% PFA for 45 minutes at room temperature. CP were then cryoprotected in 30% saccharose until CP reached the bottom (~5h) and then incubated for 4 hours with the blocking solution (PBS 2.5% BSA and 0.2% Triton). Explants were incubated overnight at 4ºC with the primary antibody GFAP, NeuN, CD11b and TTR, in the adequate dilution (Table 1). Antibodies were diluted in blocking solution. After six washes with PBS-T, the secondary antibodies were applied for three hours at room temperature in the dark. For nucleus staining, CP were incubated with Hoechst 33342 (1:1000) twenty minutes at room temperature in the dark. Finally, the coverslip was mounted with the mounting medium Entellan (Merck) and kept at -20ºC until observation under a LSM710 confocal laser scanning microscope (Carl Zeiss, Jena, Germany).

Table 1 : Primary antibodies used in immunofluorescence and Western analysis and their respective protein, dilution, technique where were used, molecular weight and company. ICC – Immunocytochemistry, WM – Whole Mount, WB – Western Blot.

Protein	Primary antibody	Dilution	Technique	Molecular weigh	Company
iNOS	iNOS rabbit polyclonal antibody	1:1000	WB	130 kDa	DB Bioscience
TTR	TTR rabbit polyclonal antibody	1:200	WB, ICC, WM	14 kDa	DAKO
β-actin	β-actin monoclonal antibody	1:20000	WB	42 kDa	Sigma Aldrich
GFAP	GFAP mouse polyclonal antibody	1:1000	WM	±50 kDa	DAKO
CD11b	Rat Anti-Integrin αMß2	1:200	WM	127 kDa	Chemicon
NeuN	NeuN mouse polyclonal antibody	1:500	WM	46 kDa	Millipore
Claudin	Claudin goat polyclonal antibody	1:50	WM and ICC	22 kDa	Santa Cruz biotechnology, Inc.

E-cadherin	E-cadherin rabbit polyclonal antibody	1:50 1:200	WM, ICC WB	135 kDa	Santa Cruz biotechnology, Inc.
ZO-1	ZO-1 goat polyclonal antibody	1:25	WM and ICC	220 kDa	Santa Cruz biotechnology, Inc.
Occludin	Occludin rabbit polyclonal antibody	1:50 1:200	WM, ICC WB	60-82 kDa	Santa Cruz biotechnology, Inc.

Table 2 : Secondary antibodies used in immunofluorescence and Western analysis and their dilution, technique were where used and company. ICC – Immunocytochemistry, WM – Whole Mount, WB – Western Blot.

Secondary antibody	Dilution	Technique	Company
Alkaline phosphatase conjugated anti-rabbit	1:20000	WB	AmershamLife Sciences
Alkaline phosphatase conjugate anti-mouse	1:20000	WB	AmershamLife Sciences
Mouse anti rat alexa 546	1:1000	WM	Invitrogen, Molecular probes
Goat anti-mouse Alexa 488	1:1000	WM, ICC	Invitrogen, Molecular Probes
Goat anti-rabbit Alexa 488	1:1000	WM, ICC	Invitrogen, Molecular Probes
Donkey anti-goat igG CFL 488	1:200	WM and ICC	Santa Cruz biotechnology, Inc.

3.4 Statistical analysis

Data are expressed as mean ± standard error of the mean (SEM) of at least three independent experiments, performed in triplicate. Differences between groups were analyzed by one-way ANOVA followed by Bonferroni's Multiple Comparison Test. Comparisons between two groups were done with Unpaired t-test. All calculations were made using GraphPah software 6.0 Demo (GraphPad Software Inc.). Statistical significance was set at $p \leq 0.05$.

Chapter 4: Results

4. Results

4.1 Effects of LPS in Choroid Plexus Epithelial Cells

In order to understand the response of CP to LPS *in vitro*, ROS and NO production were registered along a time course (0-24 hours) in CPEC and total protein content in the culture medium was evaluated.

4.1.1 ROS production

ROS production was evaluated at 1, 2, 4, 6, 8, 12, 18 and 24 hours after exposure to 0.1 μg/mL LPS. A significant increase in ROS production was observed 2 hours after LPS exposure ($p \leq 0.05$) (Figure 9) with a tendency to decrease afterwards, however without statistical significance.

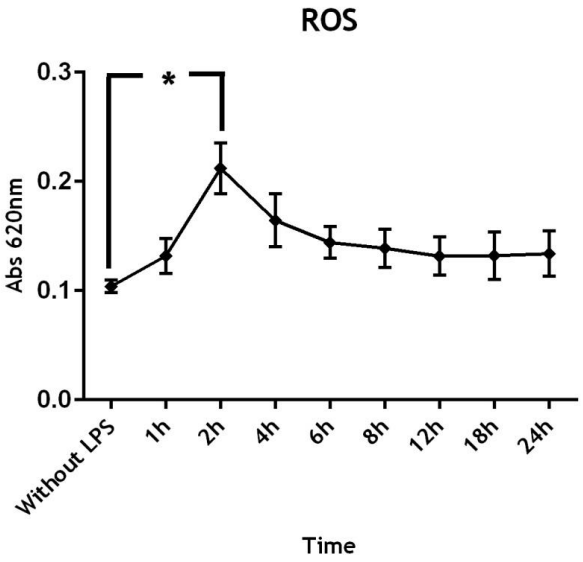

Figure 9: Time-course ROS production response to 0.1 μg/mL of LPS, in CPEC. Cells were incubated for 1, 2, 4, 6, 8, 12, 18 and 24 hours with 0.1 μg/mL of LPS. Fluorescence was measured by microplate reader spectrofluorometer at 620 nm. Data represent the mean ± SEM of three independent experiments performed in quadruplicate. Statistically significant differences among groups (*$P \leq 0.05$) were determined by one-way ANOVA and are indicated by asterisks. LPS- lipopolysaccharide, ROS- reactive oxygen species.

4.1.2 NO production

NO production was measured in the CPEC medium culture that was incubated for different times with 0.1 μg/mL of LPS. Our results suggest an increase of NO levels 2 hours after LPS exposure, with statistical significance when compared to the samples without LPS (Figure 10). These levels of NO were maintained till the end of the experiment.

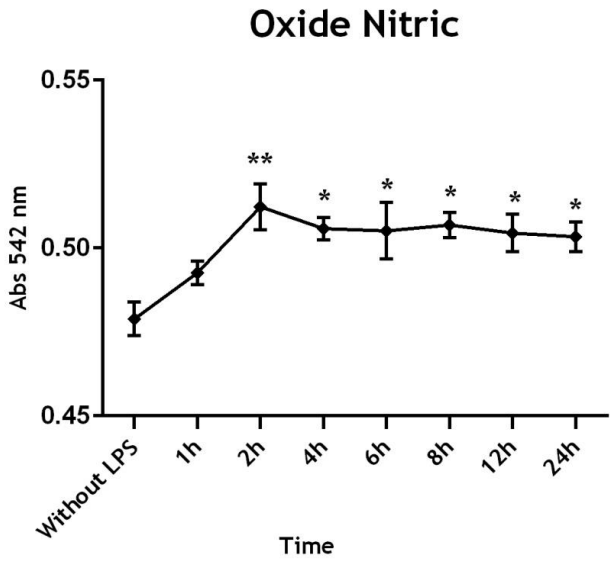

Figure 10: Time-course of oxide nitric production in response to 0.1 µg/mL of LPS in CPEC medium. Cells were stimulated for 1, 2, 4, 6, 8, 12 and 24 hours with 0.1 µg/mL of LPS. Data represent the Mean ± SEM of three independent experiments performed in quadruplicate. Statistically significant differences among groups were determined by one-way ANOVA, and are indicated by asterisks *p≤0.05, **p≤0.01, compared with control cultures (without LPS). Abs-Absorbance; LPS- lipopolysaccharide.

4.1.3 Extracellular Protein

We also assessed the levels of total protein in CPEC medium upon LPS incubation. After 1 hour of exposure to 0.1 µg/mL of LPS we observed an increase of about two fold in the protein content of the growth culture medium of CPEC. This up-regulation remained constant along the 24 hours of exposition to LPS (Figure 11).

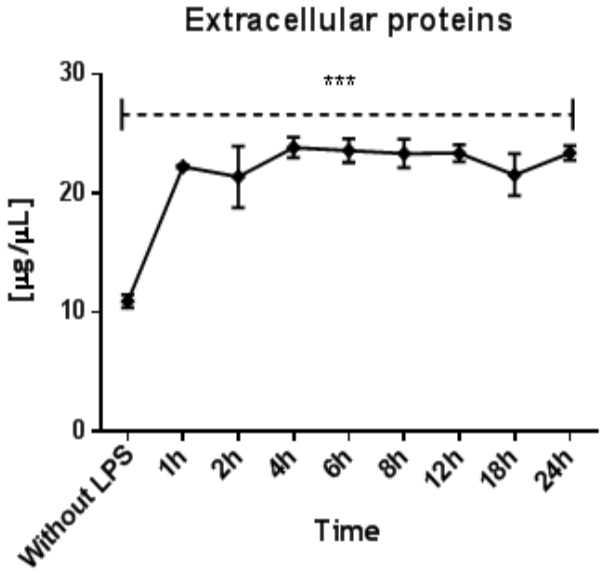

Figure 11: Quantification of extracellular proteins released from CPEC to the culture medium after incubation with 0.1 µg/mL of LPS for 24 hours. The experiment was done three times and performed in quadruplicate. Statistically significant differences among groups (***p≤0.001) were determined by one-way ANOVA and are indicated by asterisks. LPS- lipopolysaccharide.

Following this observation, we analyzed TTR and iNOS in CPEC culture medium after LPS incubation. WB did not allow iNOS detection in the cultures medium. TTR was present in culture medium at all-time points after LPS administration, but not on controls (Figure 12).

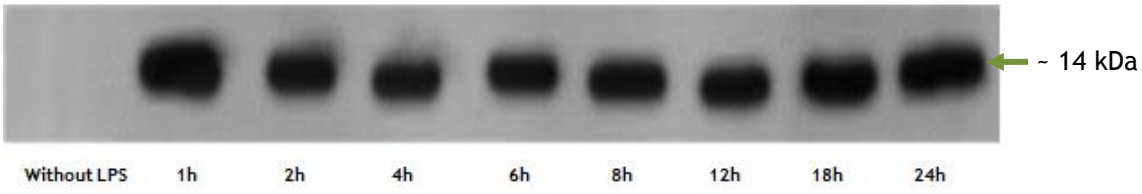

Figure 12: Western blot of TTR in extracellular medium during a time line of incubation with LPS 0.1 µg/mL. Representative image of three independent experiments. LPS- lipopolysaccharide, TTR-Transthyretin.

TTR was quantified in the culture medium showing that its levels increased significantly, 4 hours after the LPS insult decreasing afterwards (Figure 13).

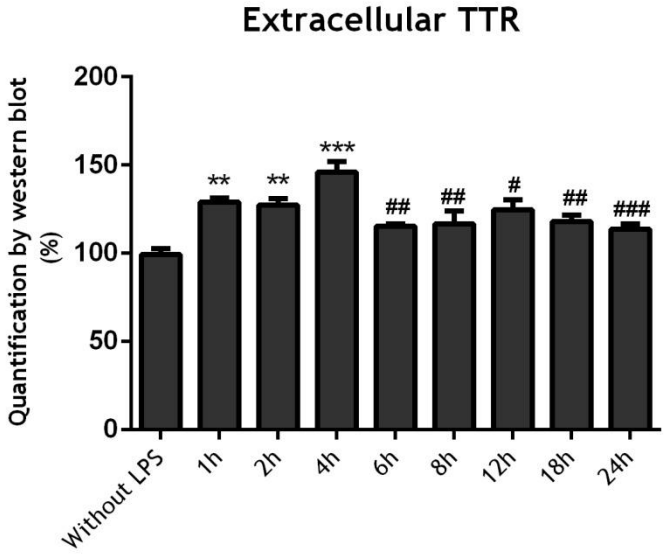

Figure 13: Quantification of TTR in CPEC medium after incubation with 0.1 µg/mL of LPS. Western blot was performed and band intensity was quantified. The experiment was done three times, performed in triplicate. Statistically significant differences among groups were determined by one-way ANOVA and are indicated by asterisks, compared to control- without LPS (**P≤0.01; ***P≤0.001); and indicated by # when compared to 4 hours (#P≤0.05; ##P≤0.01; ###P≤0.001). LPS-lipopolysaccharide, TTR-Transthyretin.

4.1.4 The effect of LPS in CPEC integrity

The impermeable BBB and BCSFB act together to protect the neuronal networks from potentially injurious agents in blood (64). To study if neuroinflammation induced by systemic LPS incorporation had effects in membrane integrity, we studied four different proteins that belong to TJ and AJ in the BCSFB. For that, we compared the effects between controls (without the neuroinflammatory agent), and cells incubated for 24 hours with 0.1 µg/mL of LPS.

The images obtained by confocal microscopy suggest that after 24 hours incubation with LPS, CPEC cells kept their morphology (Figure 14, 16, 18 and 20). Green fluorescence

quantification revealed a decrease in occludin and ZO-1 (Figure 15 and 19) with p≤0.001 and p≤0.01, respectively. No changes were found for claudin-1 and E-cadherin (Figure 17 and 21).

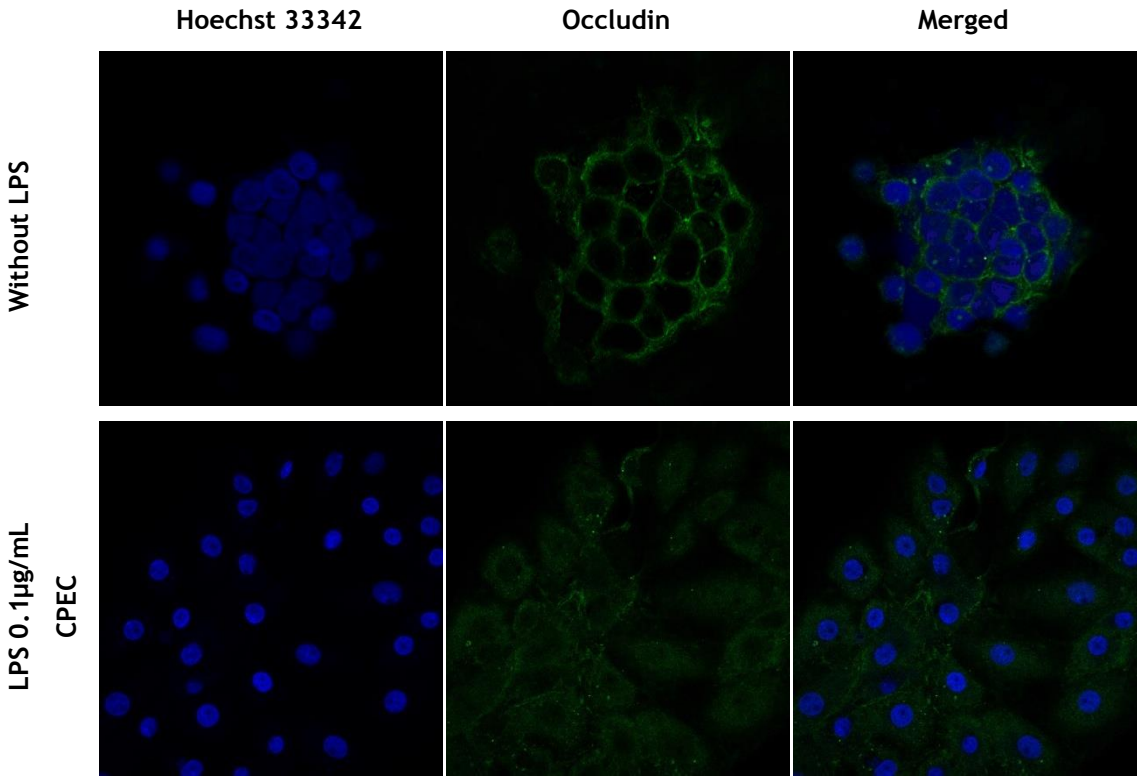

Figure 14: Effect of LPS incorporation in occludin integrity. Representative occludin immunocytochemistry confocal images from CPEC incubated with 0.1µg/mL LPS during 24 hours in newborn rats. The experiment was performed in triplicate CPEC- Choroid Plexus Epithelial Cells; LPS- lipopolysaccharide.

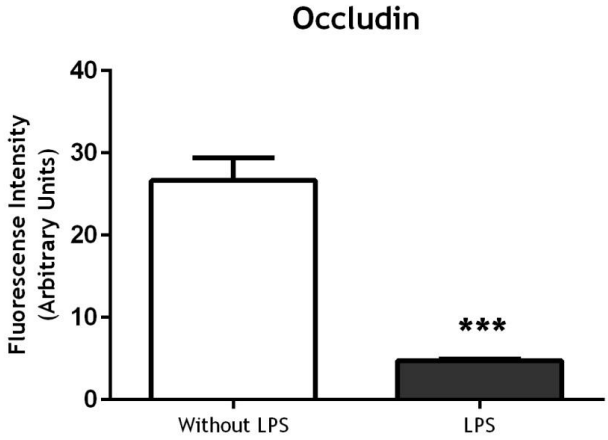

Figure 15: Effect of LPS in CPEC occludin expression. Comparison of occludin levels through measurement of mean fluorescence intensity, in CPEC treated with 0.1 µg/mL of LPS or without LPS. Data show mean values ±SEM from experiments with n=5. Statistical analysis was performed using the t-test. ***P≤0.001 as compared to control. LPS- lipopolysaccharide.

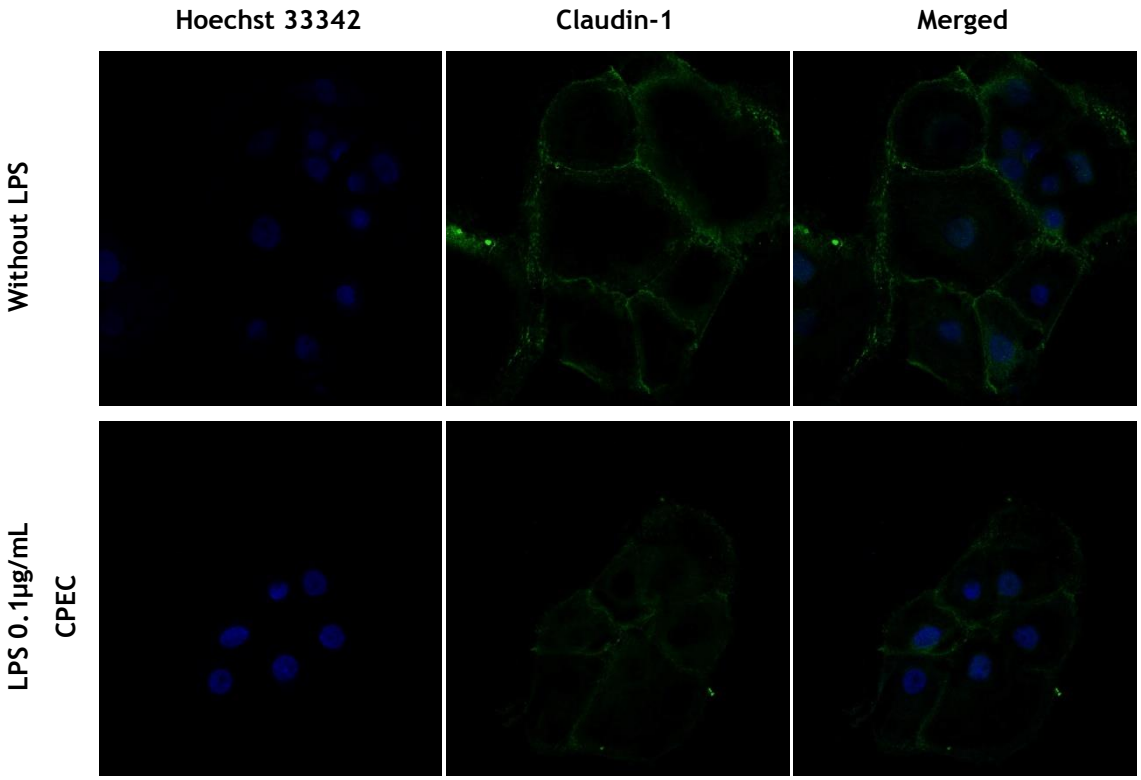

Figure 16: Effect of LPS incorporation in claudin-1 integrity. Representative claudin-1 immunocytochemistry confocal images from CPEC incubated with 0.1µg/mL of LPS during 24 hours in newborn rats. The experiment was performed in triplicate CPEC- Choroid Plexus Epithelial Cells; LPS- lipopolysaccharide.

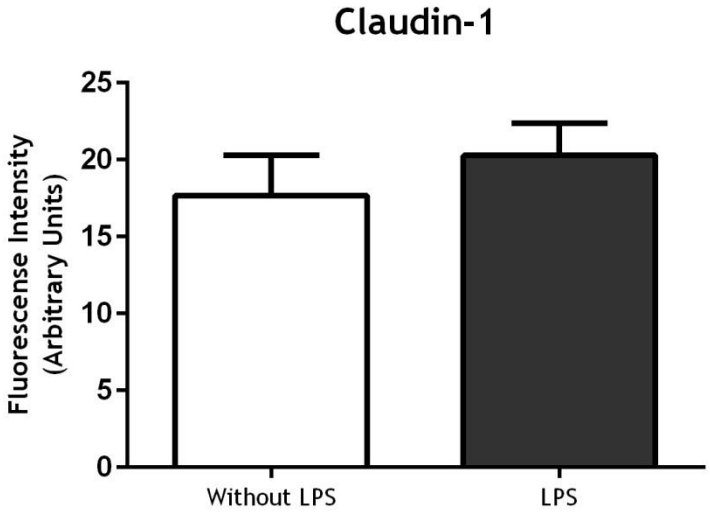

Figure 17: Effect of LPS in CPEC claudin-1 expression. Comparison of claudin-1 levels through measurement of mean fluorescence intensity, in CPEC treated with 0.1 µg/mL of LPS or without LPS. Data show mean values ±SEM from experiments with n=5. Statistical analysis was performed using the t-test. LPS- lipopolysaccharide.

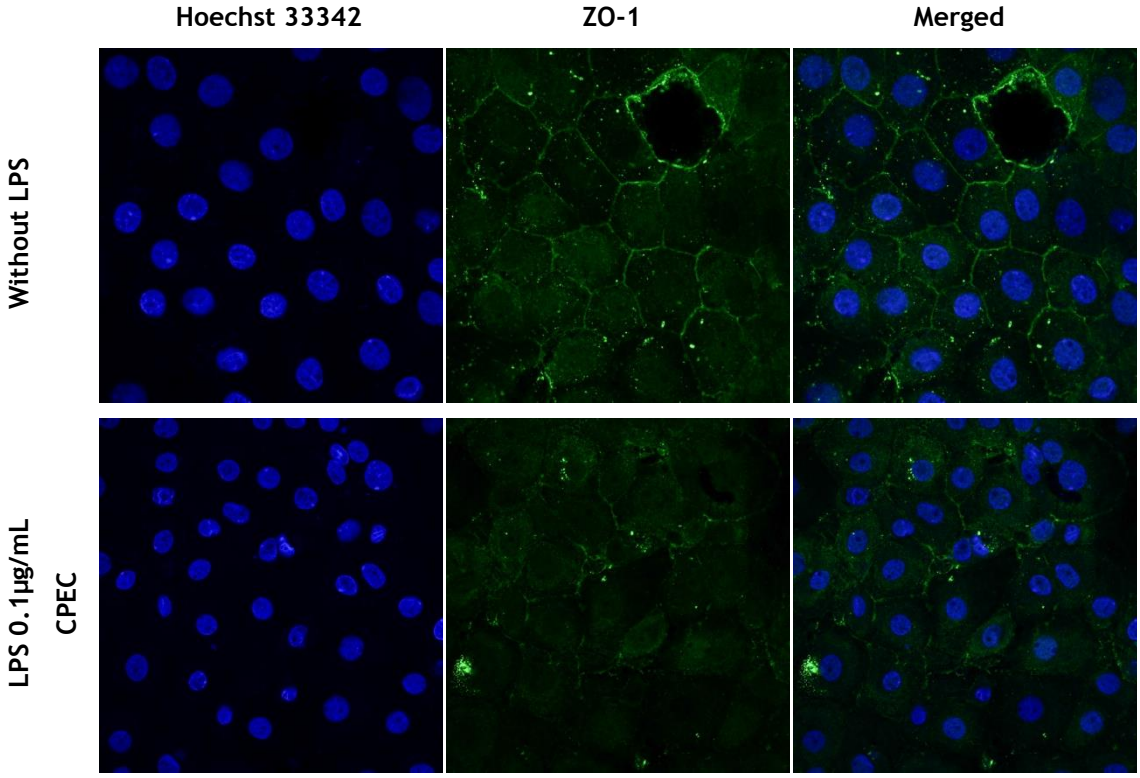

Figure 18: Effect of LPS incorporation in ZO-1 integrity. Representative ZO-1immunocytochemistry confocal images from CPEC incubated with 0.1µg/mL LPS during 24 hours in newborn rats. The experiment was performed in triplicate CPEC- Choroid Plexus Epithelial Cells; LPS-lipopolysaccharide; ZO- Zonula Occludens.

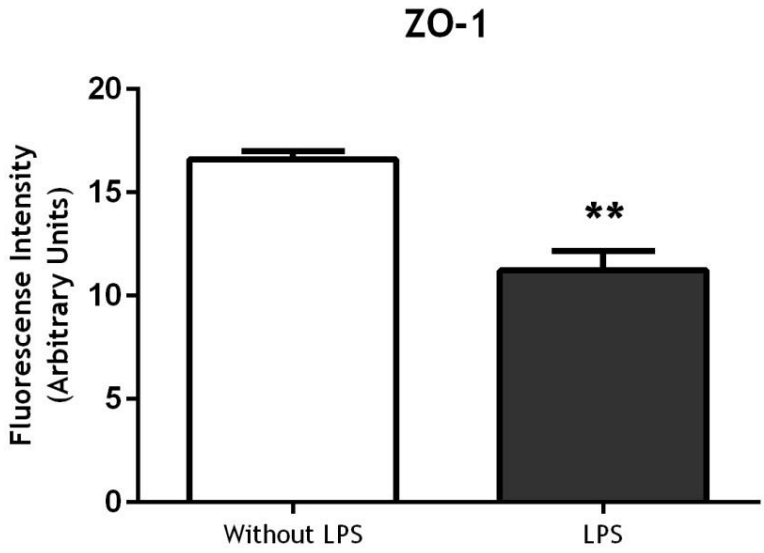

Figure 19: Effect of LPS in CPEC ZO-1 expression. Comparison of ZO-1 levels through measurement of mean fluorescence intensity, in CPEC treated with 0.1 µg/mL of LPS or without LPS. Data show mean values ±SEM from experiments with n=5. Statistical analysis was performed using the t-test. **P≤0.01 as compared to control. LPS- lipopolysaccharide; ZO- Zonula Occludens.

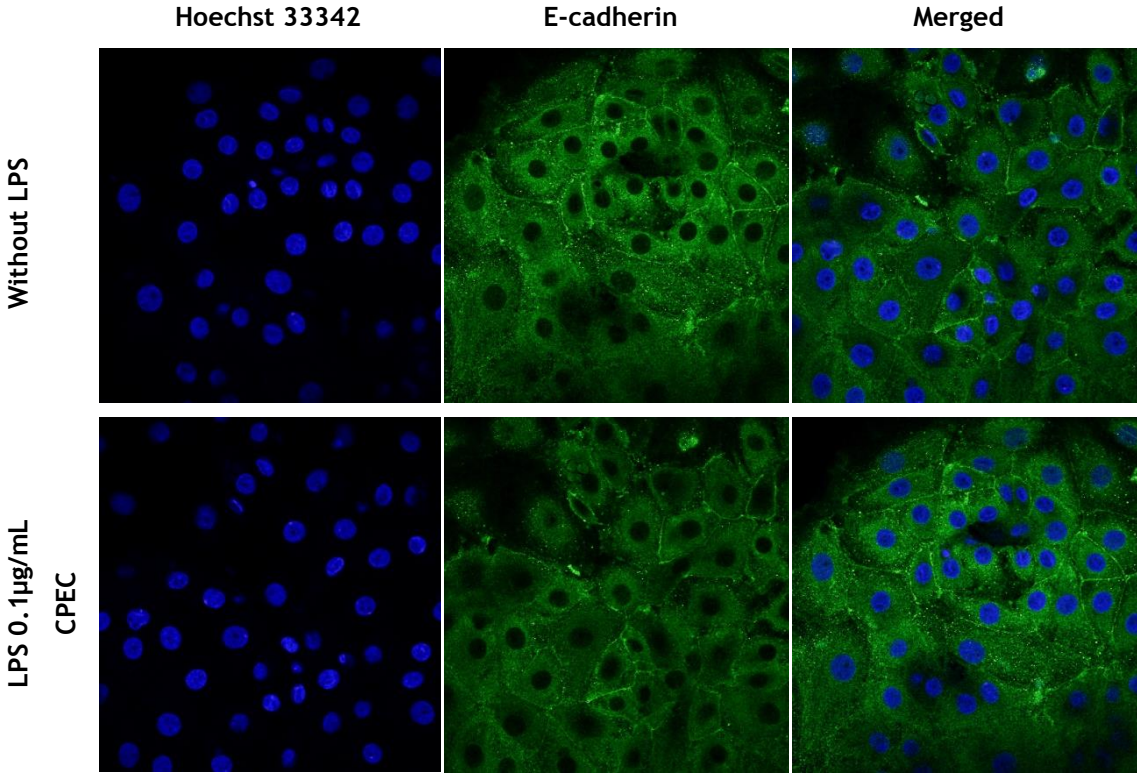

Figure 20: Effect of LPS incorporation in E-cadherin integrity. Representative E-cadherin immunocytochemistry confocal images from CPEC incubated with 0.1µg/mL LPS during 24 hours in newborn rats. The experiment was performed in triplicate CPEC- Choroid Plexus Epithelial Cells; LPS- lipopolysaccharide.

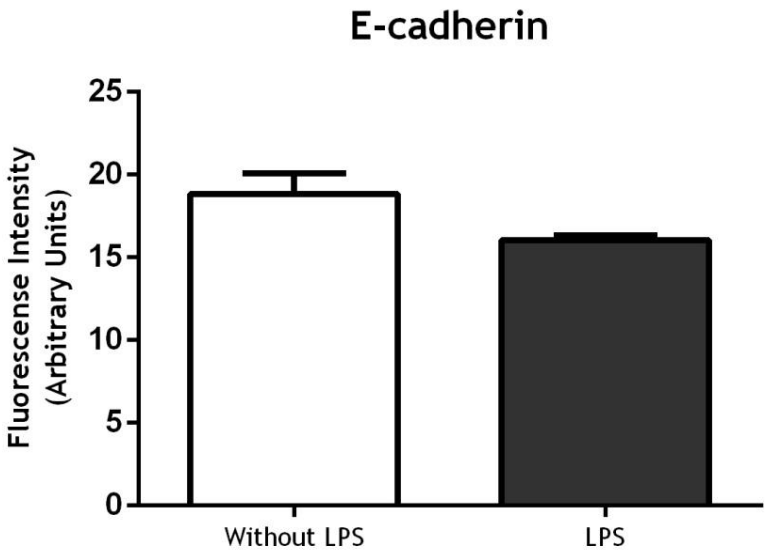

Figure 21: Effect of LPS in CPEC E-cadherin expression. Comparison of E-cadherin levels through measurement of mean fluorescence intensity, in CPEC treated with 0.1 µg/mL of LPS or without LPS. Data show mean values ±SEM from experiments with n=5. Statistical analysis was performed using the t-test. LPS- lipopolysaccharide.

4.2. Effect of LPS in CP explants

To understand the extent of the effects of LPS in CP explants collected from newborn animals and 21 days rats, we analyzed ROS production, using WM for CD11b, GFAP and NeuN. For 21 days rats we compared TTR levels and iNOS in the CP by WB.

4.2.1 ROS production

Incubation of CP explants with 0.1 µg/mL of LPS for 2 hours resulted in an increase in ROS production in newborn and 21 days rats (Figure 22 and 23). This increase was remarkably higher in the later animals.

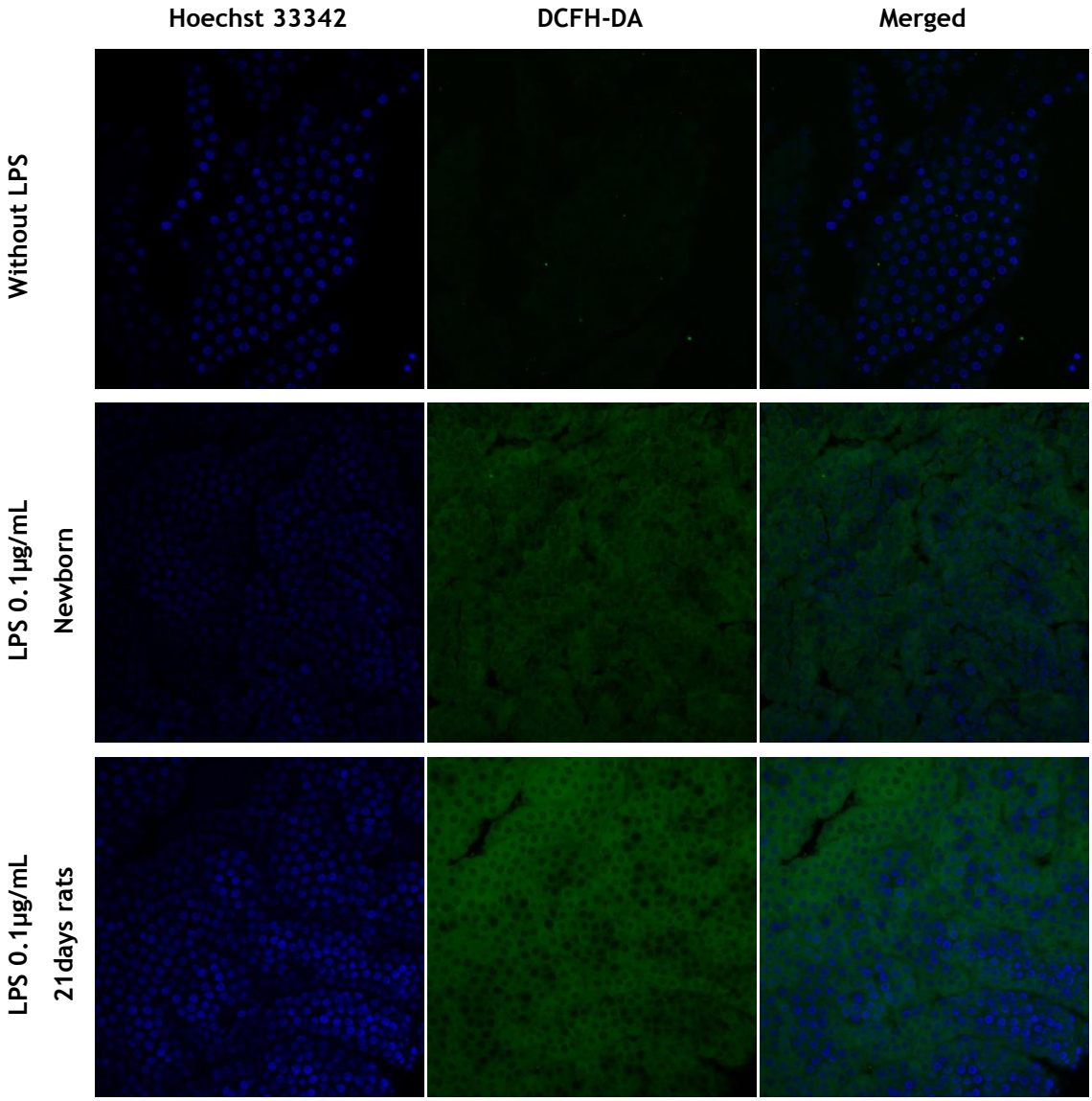

Figure 22: ROS production after 2 hours of 0.1 µg/mL of LPS incorporation. Representative image of five independent experiments. DCFH-DA- dichloro-dihudro-fluorescein-diacetate LPS- lipopolysaccharide

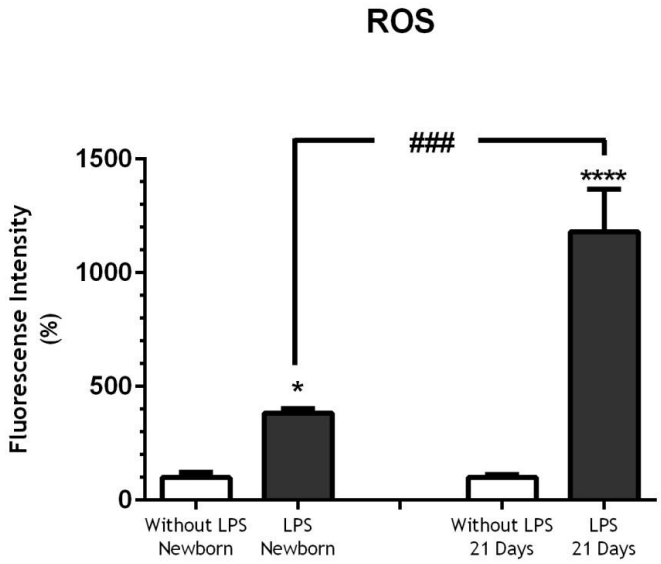

Figure 23: ROS production after 2 hours of 0.1 µg/mL of LPS incorporation in newborn and 21 days rats. Graphic represents fluorescence quantification of CP labeled with DCFHA-DA 2 hours after 0.1 µg/mL of LPS incubation. Data show mean values ±SEM from experiments with n=5. Statistical analysis was performed using the ANOVA. LPS vs. without LPS (*P≤0.05; ****P≤0.0001); newborn vs. 21 day rats (###P≤0.001). LPS- lipopolysaccharide, ROS- Reactive Oxygen Species.

4.2.2 TTR, CD11b, GFAP and NeuN expression

To better understand the effects of systemic LPS on CP, we incubated CP explants from newborn and 21 days rats with 0.1 µg/mL of LPS during 48 hours and performed WM for TTR, CD11b, GFAP and NeuN. After fluorescence quantification with ZEN software, treatment with LPS revealed a significant change in neuroinflammation and neurogenesis markers. LPS treatment during 48 hours did not impair TTR expression (Figure 24 and 25), but displayed an increase in CD11b expression (Figure 26 and 27) and GFAP (Figure 30 and 31) and a decrease in NeuN expression (Figure 29 and 30).

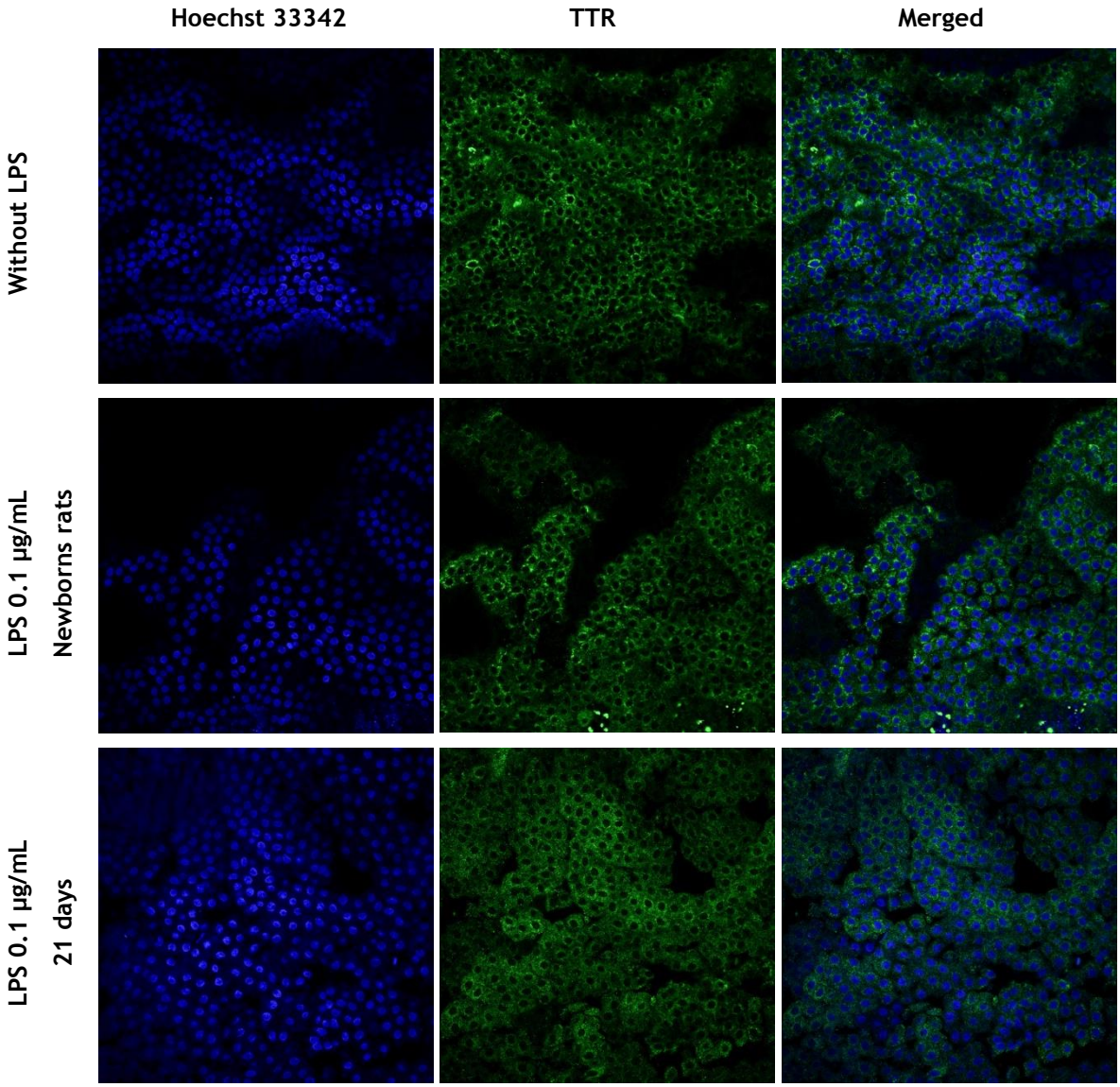

Figure 24: Representative confocal images of LPS effects on CP TTR expression. Image represent TTR expression in CP explants after incubation with 0.1 µg/mL of LPS for 48 hours in newborn and 21 days rats. LPS-lipopolysaccharide, TTR- Transthyretin.

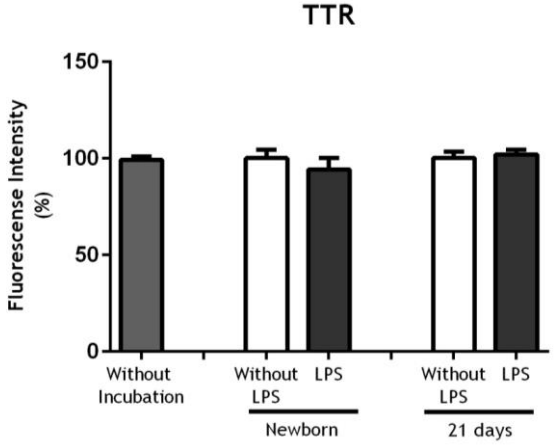

Figure 25: Effect of LPS on CP TTR expression. Comparison of TTR levels through measurement of mean fluorescence intensity, with 0.1 µg/mL of LPS or without LPS in CP explants from newborn and 21 days rats. Data show mean values ±SEM from experiments with n=5. Statistical analysis was performed using the t-test LPS- lipopolysaccharide, TTR- Transthyretin.

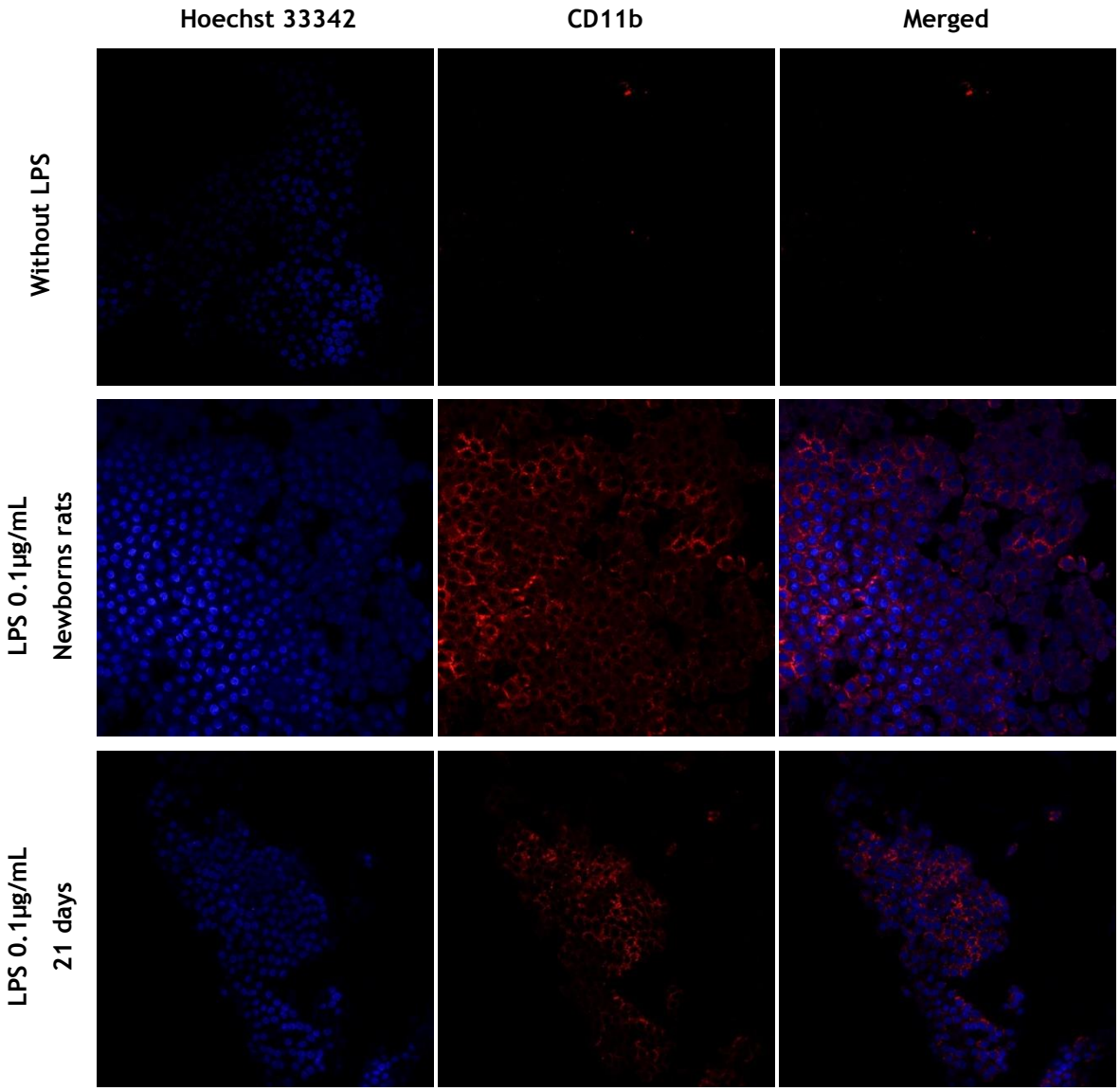

Figure 26: Representative confocal images of LPS effects on CP CD11b expression. Images represent CD11b expression in CP explants after incubation with 0.1 µg/mL of LPS for 48 hours in newborn and 21 days rats. LPS-lipopolysaccharide.

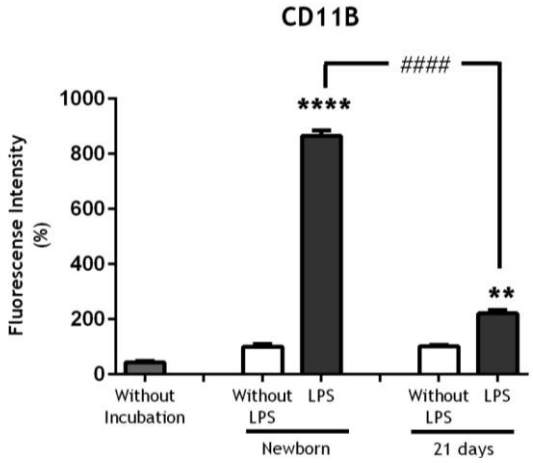

Figure 27: Effect of LPS on CP CD11b expression. Comparison of CD11b levels through measurement of mean fluorescence intensity, with 0.1 µg/mL of LPS or without LPS in CP explants from newborn and 21 days rats. Data show mean values ±SEM from experiments with n=5. Statistical analysis was performed using the ANOVA. LPS vs. Without LPS (****P≤0.0001 and **P≤0.01); newborn vs. 21days rats (####P≤0.0001). LPS- lipopolysaccharide.

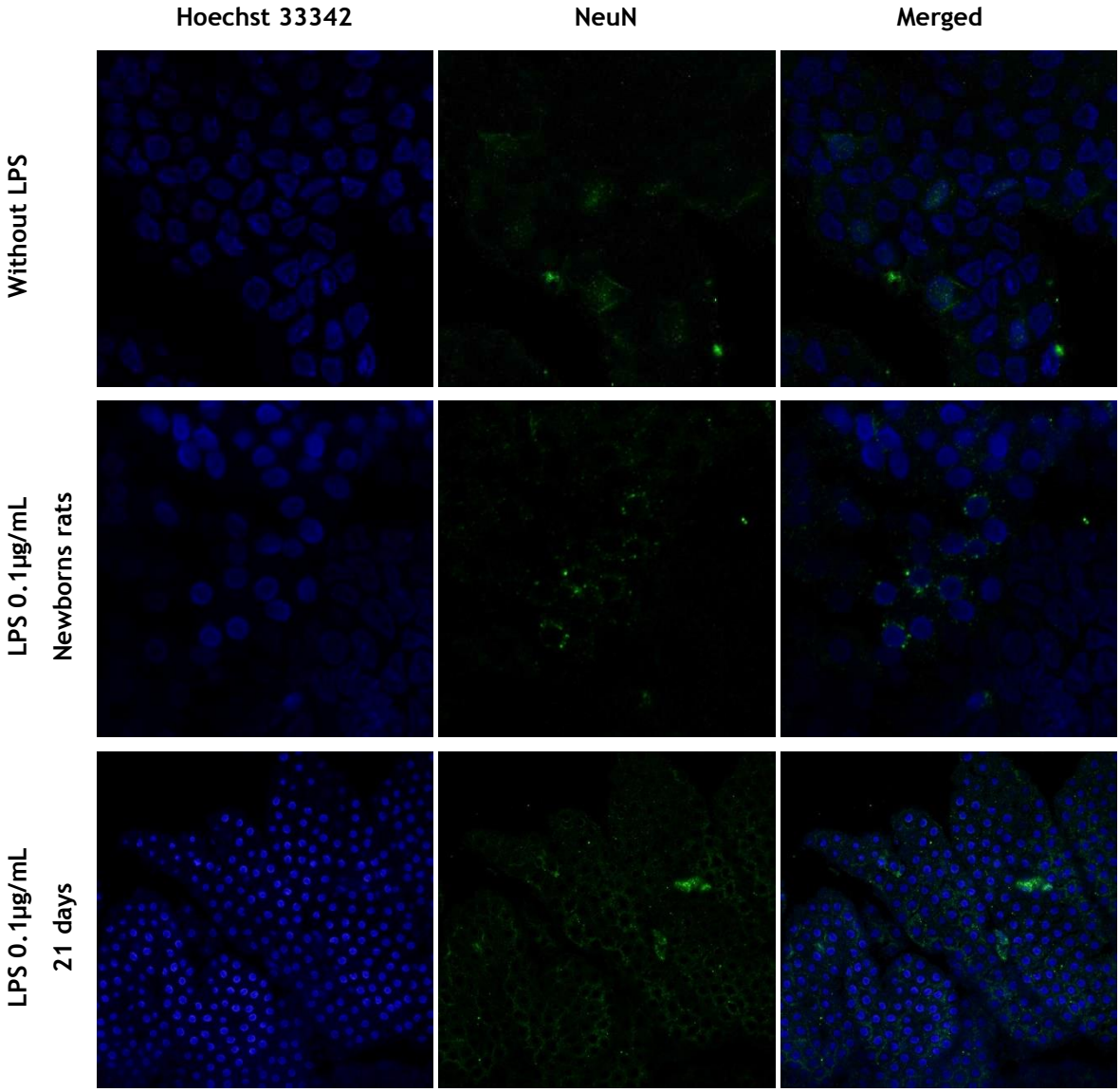

Figure 28: Representative confocal images of LPS effects on CP NeuN expression. Images represent NeuN expression in CP explants after incubation with 0.1 µg/mL of LPS for 48 hours in newborn and 21 days rats. LPS-lipopolysaccharide, NeuN- Neuronal Nuclear Protein.

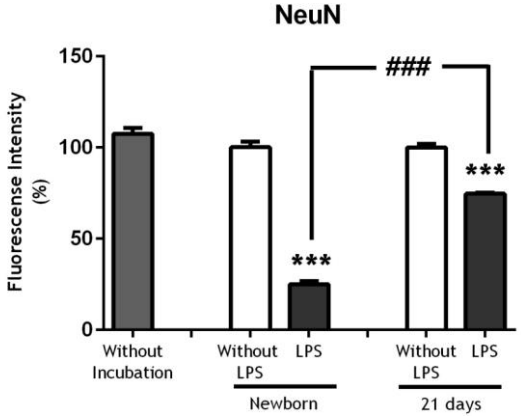

Figure 29: Effect of LPS on CP NeuN expression. Comparison of NeuN levels through measurement of mean fluorescence intensity, with 0.1 µg/mL of LPS or without LPS in CP explants from newborn and 21 days rats. Data show mean values ±SEM from experiments with n=5. Statistical analysis was performed using the ANOVA. LPS vs. without LPS (***P≤0.001); newborn vs. 21 days rats (###P≤0.001). LPS-lipopolysaccharide, NeuN- Neuronal Nuclear Protein.

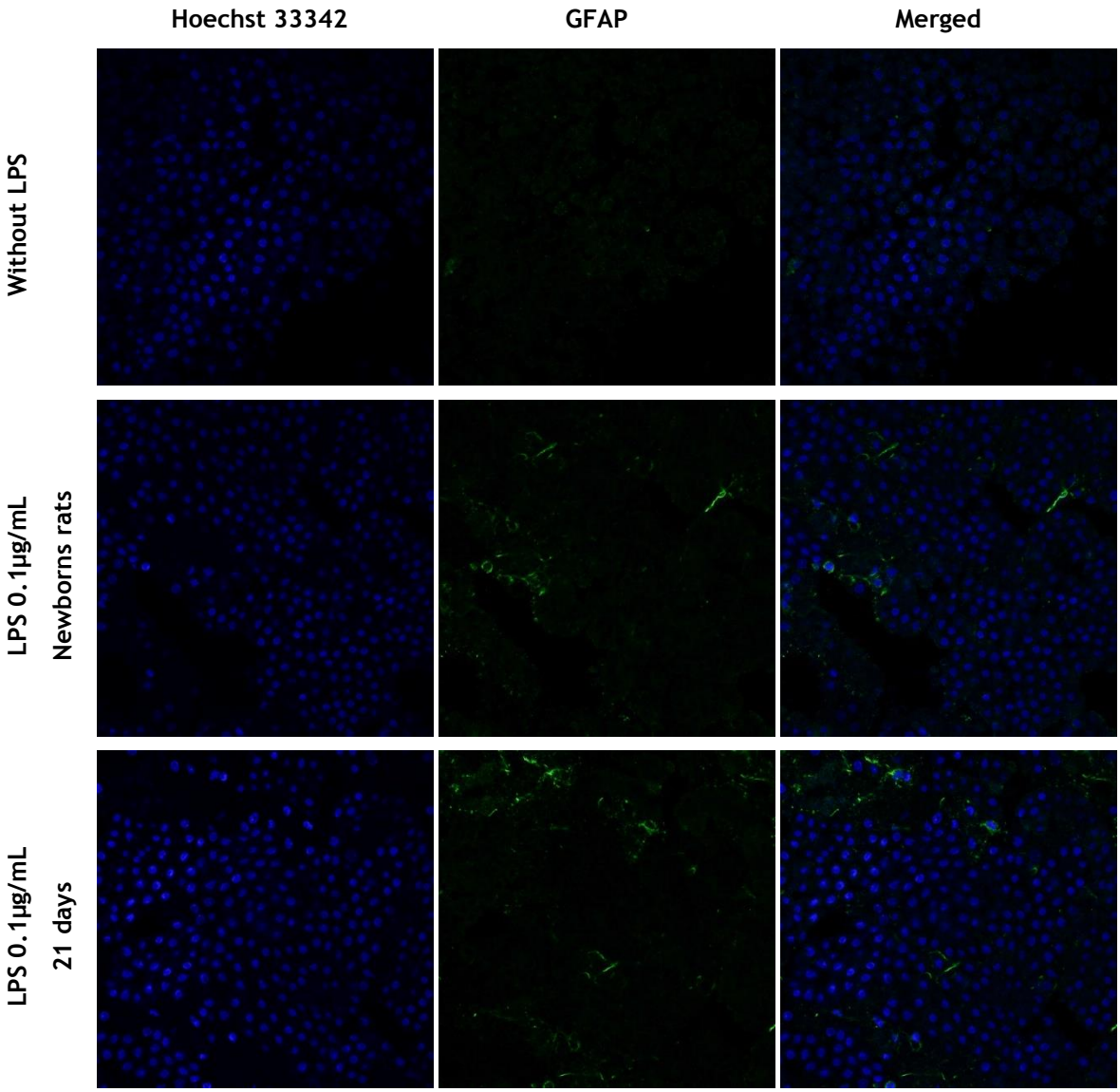

Figure 30: Representative confocal images of LPS effects on CP GFAP expression. Image represent GFAP expression in CP explants after incubation with 0.1 µg/mL of LPS for 48 hours in newborn and 21 days rats. LPS-lipopolysaccharide, GFAP- Glial Fibrillary Acidic Protein.

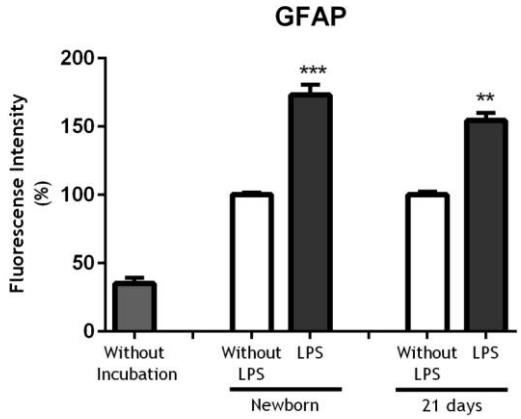

Figure 31: Effect of LPS in CP *ex vivo* GFAP expression. Comparison of GFAP levels through measurement of mean fluorescence intensity, with 0.1 µg/mL of LPS or without LPS in CP explants from newborn and 21 days rats. Data show mean values ±SEM from experiments with n=5. Statistical analysis was performed using the ANOVA. LPS vs. without LPS (**P≤0.01; ***P≤0.001). LPS- lipopolysaccharide, GFAP- Glial Fibrillary Acidic Protein.

4.2.3 Western Blot

4.2.3.1 TTR

TTE expression was also analyzed in CP explants exposed to LPS. WB analysis was performed on total protein extracted from explants of 21 days rats after incubation with 0.1 µg/mL of LPS for 48 hours, and control explants that were incubated with vehicle only (Figure 32). After quantification of results obtained by WB, from four independent experiments, it was possible to verify that the expression of TTR in CP explants remains the same with or without LPS treatment (Figure 33).

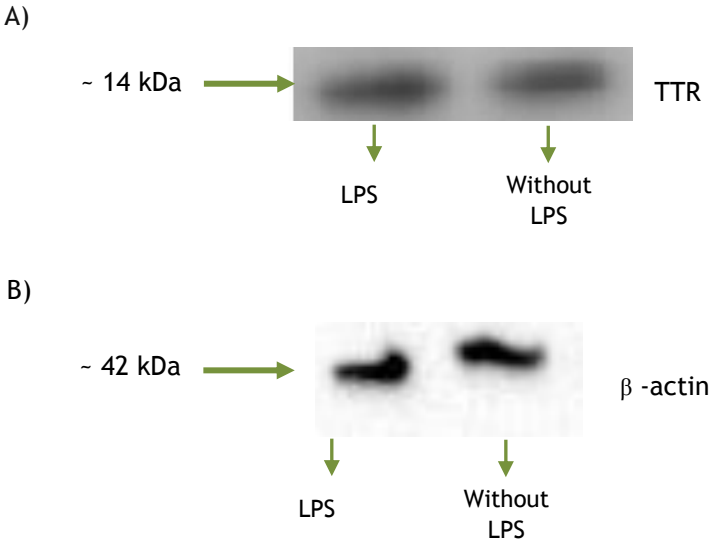

Figure 32: Representative WB image of TTR. Explants of 21 days rats were incubated with 0.1 µg/mL of LPS for 48 hours, subsequently the protein was extracted and WB performed. A) Show a band of ~14 kDa, corresponding to monomer form of TTR. B) Show a band of ~42 kDa, corresponding to ß-actin.

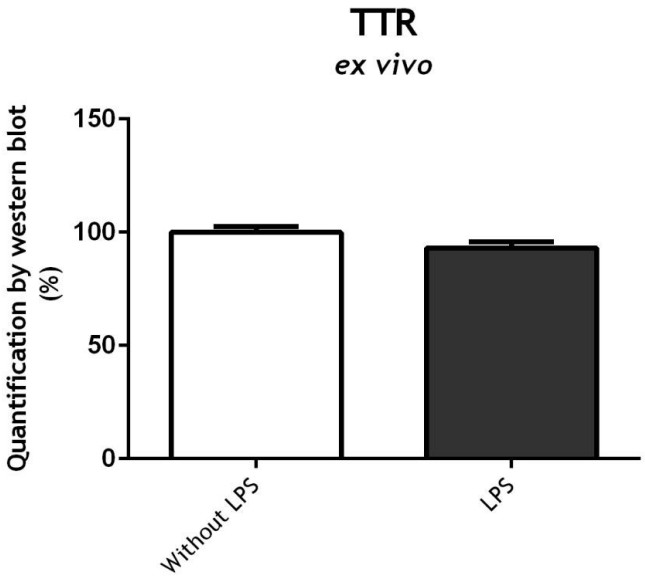

Figure 33: Quantification of expression of TTR in explants of 21 days rats incubated with 0.1 µg/mL of LPS. The graph is the result of quantify four independent experiments. Data show mean values ±SEM from experiments with n=4. Statistical analysis was performed using the t-test. LPS- lipopolysaccharide, TTR- Transthyretin

4.2.3.2 iNOS

To study if LPS increase or induce iNOS expression in CP, we performed a WB. CP explants of s 21 days rats were incubated for 48 hours with LPS. In figure 34, we observe the presence of a band that corresponds to iNOS (130 kDa) in incubated samples, while the control explants without incubation with LPS did not show any band (Figure 34). Accordingly band quantification showed that LPS insult induces CP to express the iNOS protein (Figure 35).

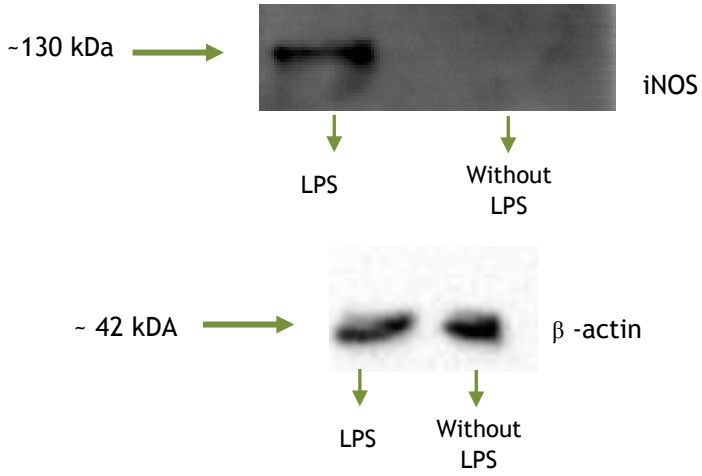

Figure 34: Representative WB image of iNOS. Explants of rats with 21 days were incubated with 0.1 µg/mL of LPS for 48 hours, subsequently the protein was extracted and WB performed. A) Show a band of ~130 kDa, corresponding to iNOS. B) Show a band of ~42 kDa, corresponding to ß-actin.

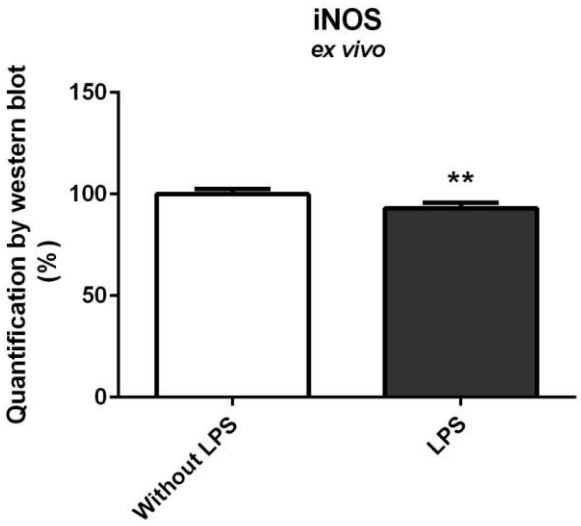

Figure 35: Quantification of expression of iNOS in explants of rats with 21 days incubated with 0.1 µg/mL of LPS. Data show mean values ±SEM from experiments with n=4. Statistical analysis was performed using the t-test. LPS vs. without LPS (**P≤0.01). iNOS- inducible nitric oxide synthase; LPS- lipopolysaccharide.

4.2.4 The effect of LPS in CPEC integrity

BCSFB integrity of newborn rat CP explants, after treatment with LPS, was accessed by WM through the measurement of expression levels of some membrane proteins found at TJ and AJ, namely occludin and E-cadherin (Figure 36 and 38). LPS did not change membrane protein expression in CP explants (Figure 37 and 39).

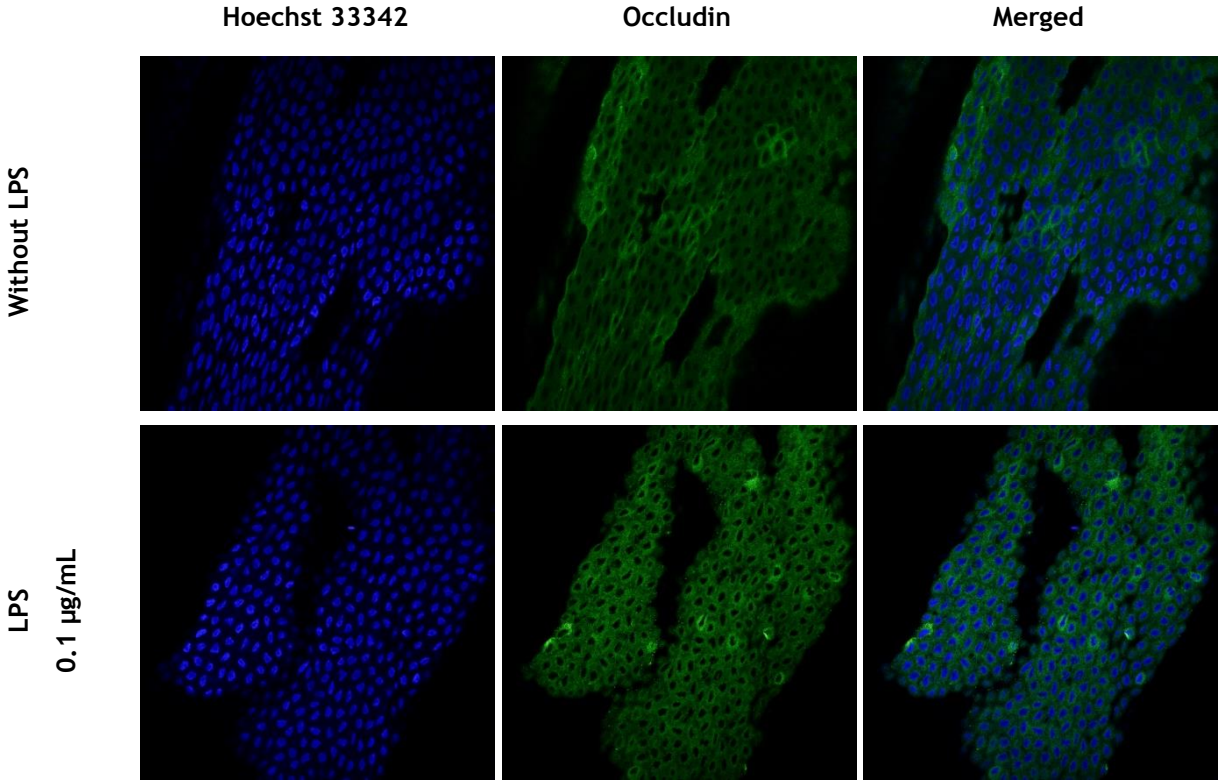

Figure 36: Representative confocal images of LPS effects on CP occludin expression. Images represent occludin expression in CP explants after incubation with 0.1 µg/mL for 24 hours in newborn rats. LPS-lipopolysaccharide.

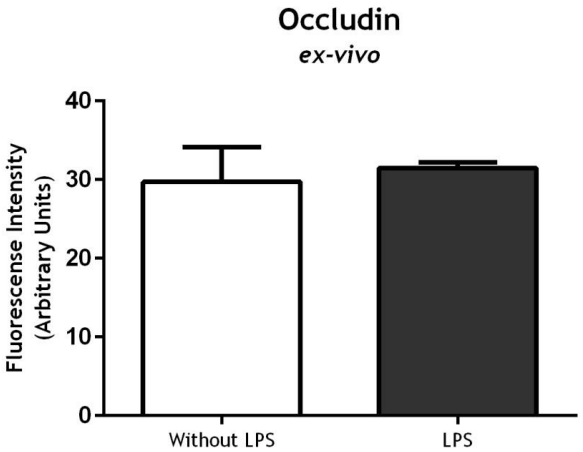

Figure 37: Effect of LPS in CP occludin expression. Comparison of occludin levels through measurement of mean fluorescence intensity, in CP explants from newborn rats incubated with 0.1 µg/mL of LPS or without LPS. Data show mean values ±SEM from experiments with n=3. Statistical analysis was performed using the t-test. LPS- lipopolysaccharide.

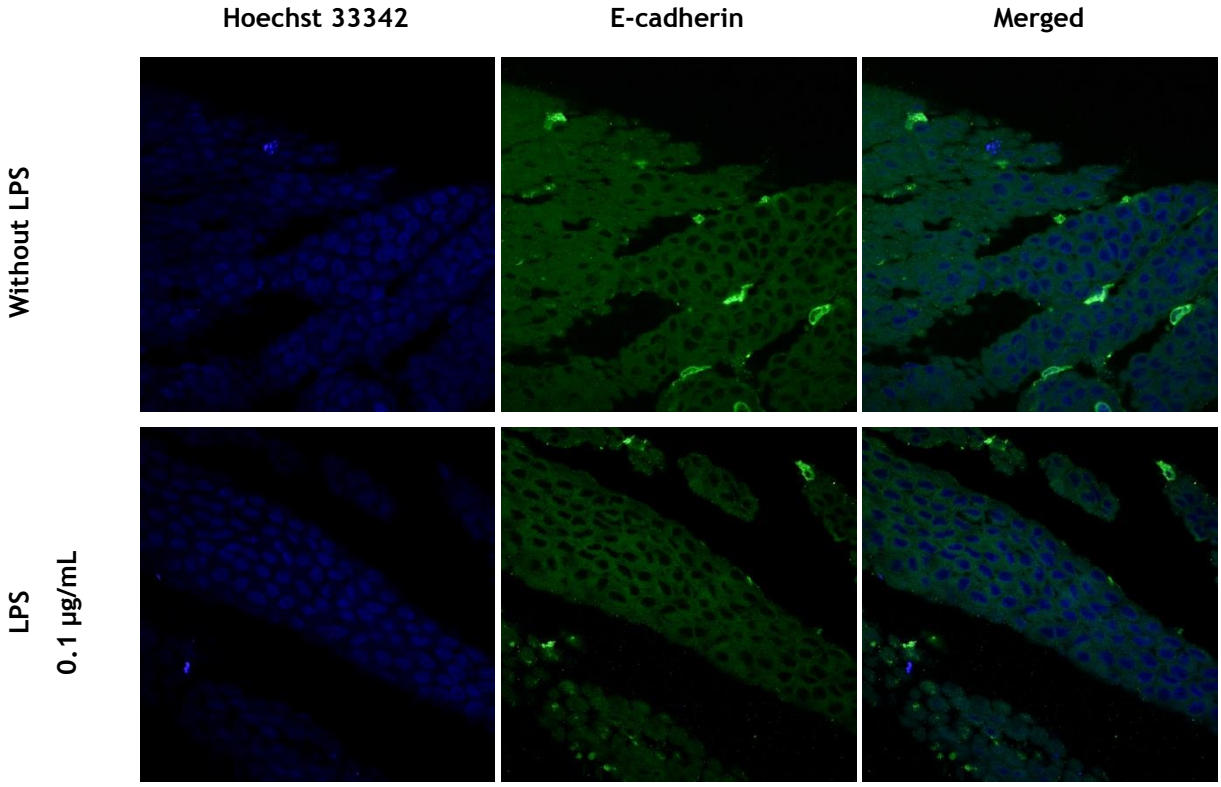

Figure 38: Representative confocal images of LPS effects on CP E-cadherin expression. Images represent E-cadherin expression in CP explants after incubation with 0.1 µg/mL for 24 hours in newborn rats. LPS-lipopolysaccharide.

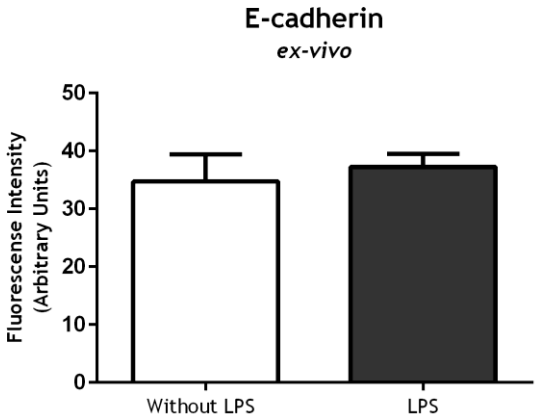

Figure 39: Effect of LPS in CP E-cadherin expression. Comparison of E-cadherin levels through measurement of mean fluorescence intensity, in CP explants from newborn rats incubated with 0.1 µg/mL of LPS or without LPS. Data show mean values ±SEM from experiments with n=3. Statistical analysis was performed using the t-test. LPS- lipopolysaccharide.

4.3 Study of the response of CP *in vivo* to a LPS insult

In order to study possible alterations in TTR, iNOS, E-cadherin and Occludin expression in CP during aging, mice at different ages (1, 3 and 9 months) were injected with 1.0 mg/kg of LPS and sacrificed 7 hours after. For that, protein expression was evaluated by WB. Resulting blots were analyzed by densitometry and quantified.

4.3.1 TTR

As previously mentioned, TTR is the major protein secreted by the CP, which gives it a high interest when the goal is analyze possible changes in protein synthesis. For TTR expression study in animals of different ages with and without incubation of LPS, it was possible to verify that LPS incubation had no significant effect on TTR expression. However, through the analysis of the figure 41 we can observe a decrease in the expression of TTR over age, with a significant difference between animals with 1 month of 9 months (P≤0.05) (figures 40, 41).

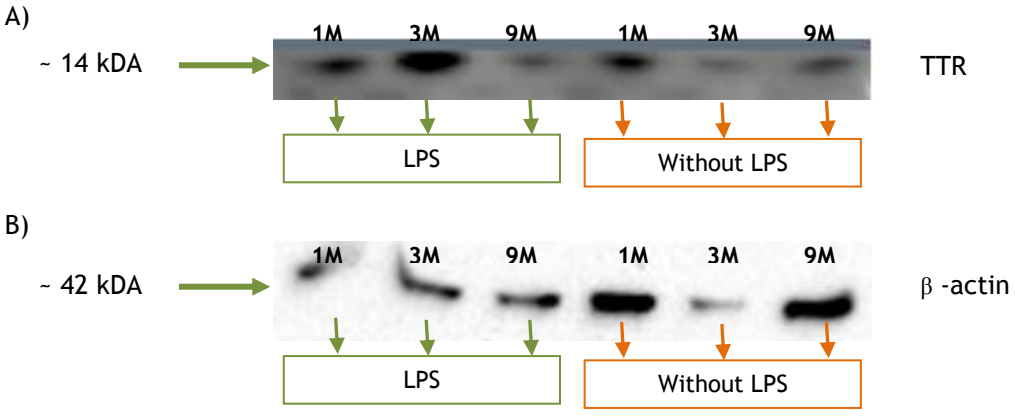

Figure 40: Representative WB image of TTR. Mice were injected with 1.0 mg/kg of LPS and euthanized 7 hours after injection, subsequently the protein was extracted and WB performed. A) Show a band of ~14 kDa, corresponding to TTR. B) Show a band of ~42 kDa, corresponding to ß-actin. 1M – 1 month; 3M – 3 months; 9M- 9 months; LPS- lipopolysaccharide; TTR- Transthyretin.

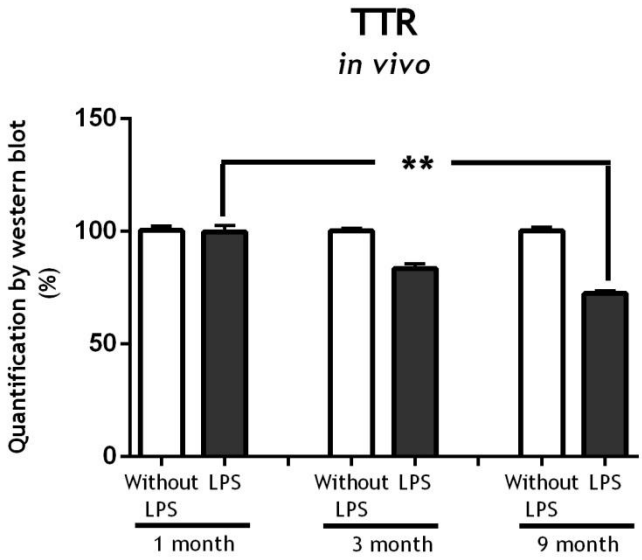

Figure 41: Quantification of TTR expression in explants collected from 1, 3 and 9 months mice injected with 1.0 mg/kg of LPS. Data show mean values ±SEM from experiments with n=6. Statistical analysis was performed using the t-test. 1month vs. 3 months (**P≤0.01). LPS- lipopolysaccharide; TTR- Transthyretin

4.3.2 iNOS

iNOS expression analysis, showed that in CP of mice injected with 1.0 mg/kg of LPS, while in control animals was not observed this presence. Changes resulting from age were not possible to observe, considering that only two experiments were performed.

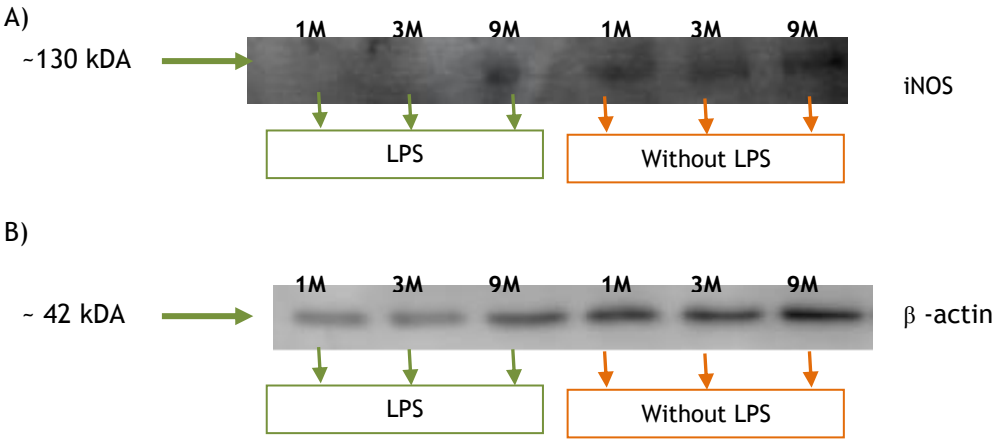

Figure 42: Representative WB image of iNOS. Mice were injected with 1.0 mg/kg of LPS and euthanized 7 hours after injection, subsequently the protein was extracted and WB performed. A) Show a band of ~130 kDa, corresponding to iNOS. B) Show a band of ~42 kDa, corresponding to ß-actin. 1M – 1 month; 3M – 3 months; 9M- 9 months; LPS- lipopolysaccharide.

4.3.3 E-cadherin and occludin

Western blot technique was performed to confirm the expression of occludin and E-cadherin, proteins in mice CP and the influence of LPS in their expression. Representative images of WB performed, can be observed in Figure 43 and 44, but as only two experiments were carried, it was not possible to deduce if acute neuroinflammatory insult or age might influence the expression of proteins of membrane integrity.

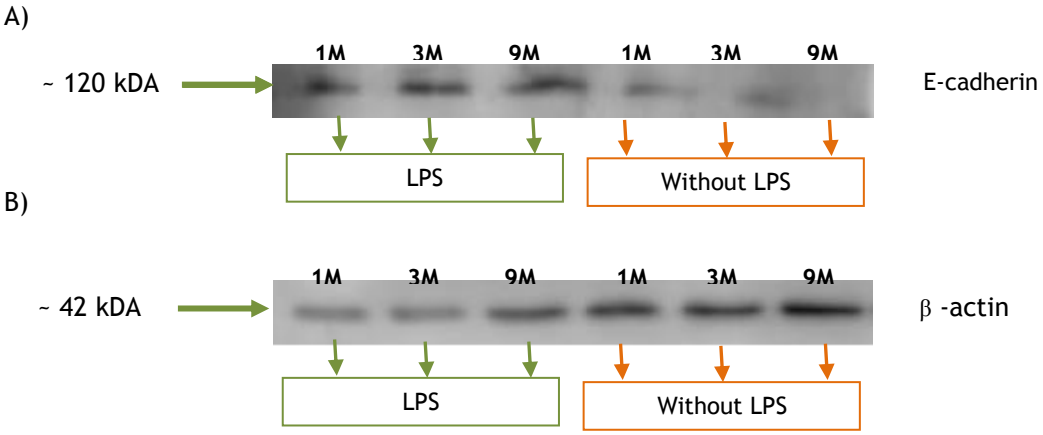

Figure 43: Representative WB image of E-cadherin. Mice were injected with 1.0 mg/kg of LPS and euthanized 7 hours after injection, subsequently the protein was extracted and western blot performed. A) Show a band of ~120 kDa, corresponding to E-cadherin. B) Show a band of ~42 kDa, corresponding to ß-actin. 1M – 1 month; 3M – 3 months; 9M- 9 months; LPS- lipopolysaccharide.

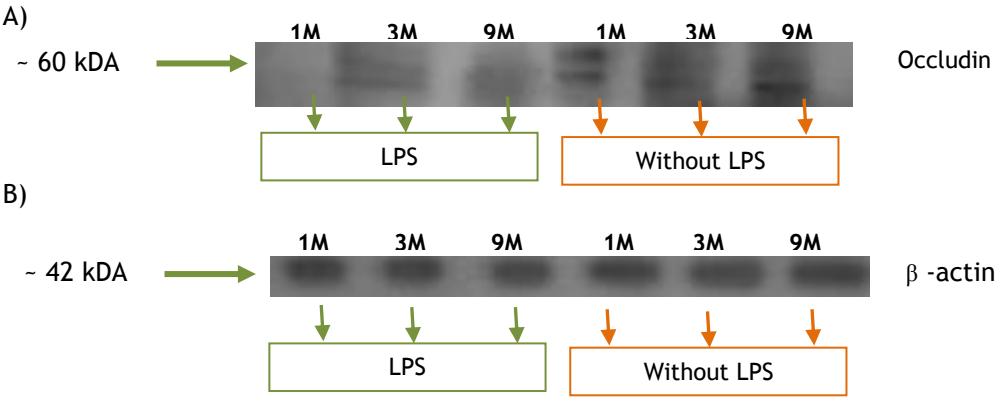

Figure 44: Representative WB image of occludin. Mice were injected with 1.0 mg/kg of LPS and euthanized 7 hours after injection, subsequently the protein was extracted and WB performed. A) Show a band of ~60 kDa, corresponding to occludin. B) Show a band of ~42 kDa, corresponding to ß-actin. 1M – 1 month; 3M – 3 months; 9M- 9 months; LPS- lipopolysaccharide.

4.4 Study of neurogenesis in CP *in vivo* in response to a LPS insult

To understand the effects of systemic LPS on the potential of CP cells to differentiate in neurons and astrocytes, mice (1 and 3 month old) were injected with 1 mg/kg of LPS and WM was performed for TTR, CD11b, NeuN and GFAP, 28 days after the LPS injection. After fluorescence quantification with ZEN software, treatment with LPS revealed a significant change in the markers analyzed.

4.4.1 TTR

Quantification analysis of TTR expression in CP of mice with 1 month and 3 month didn't showed significant changes in TTR expression (Figure 45 and 46).

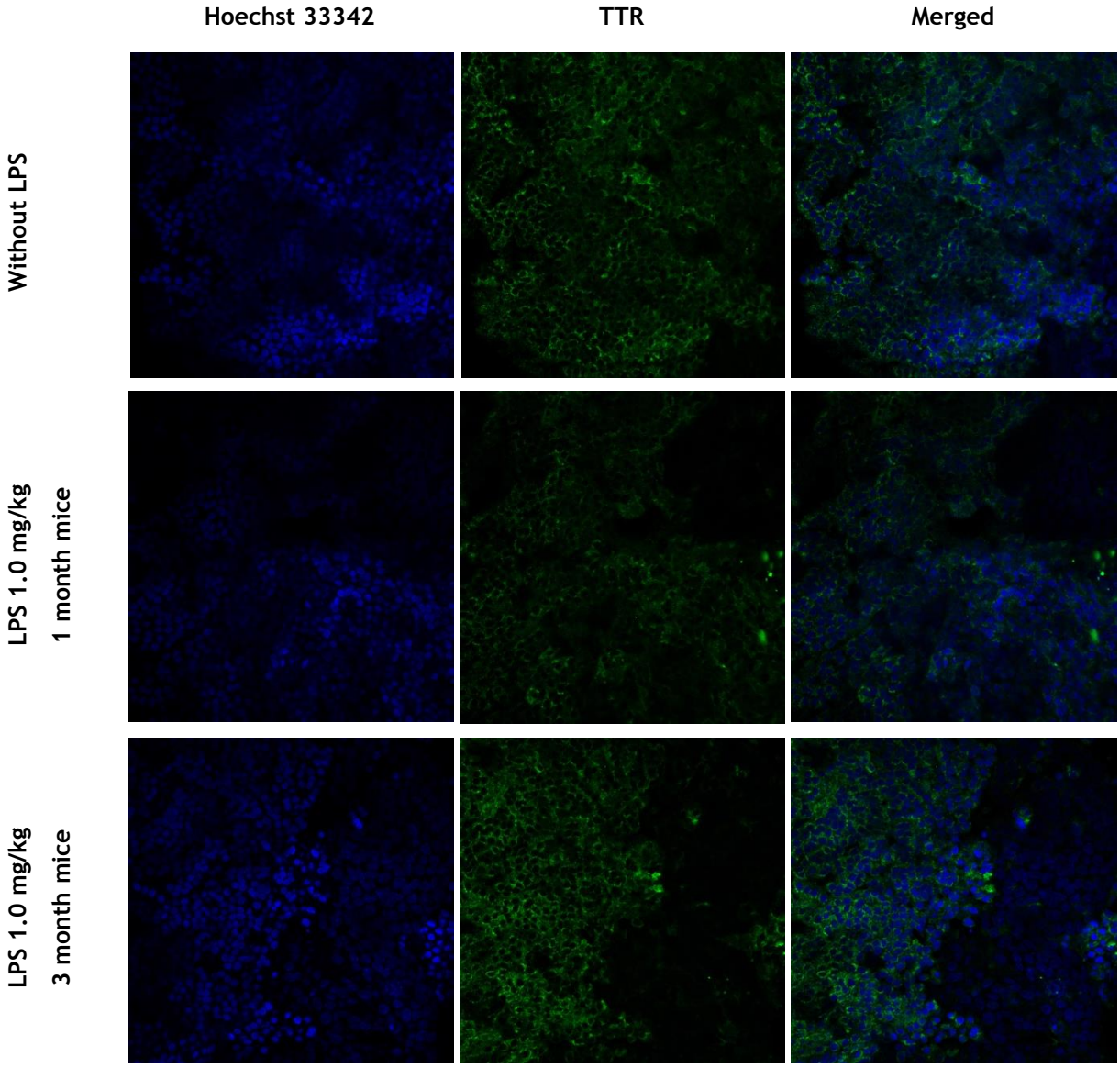

Figure 45: Representative confocal images of LPS effects *in vivo* in CP TTR expression. Image represent TTR expression in CP explants 28 days after 1.0 mg/kg of LPS intraperitoneal administration in 1 and 3 month mice. LPS-lipopolysaccharide, TTR- Transthyretin.

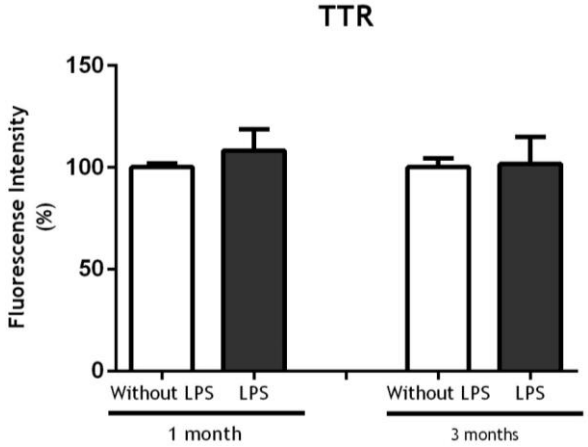

Figure 46: Effect of LPS in CP TTR expression. Comparison of TTR levels through measurement of mean fluorescence intensity, in CP explants from 1 month and 3 months mice injected with 1.0 mg/kg of LPS or without LPS. Data show mean values ±SEM from experiments with n=4. Statistical analysis was performed using the ANOVA. LPS- lipopolysaccharide, TTR- Transthyretin.

4.4.2 CD11b

Looking figure 47, it is possible to report that impairment in CD11b expression occurs 28 days after LPS injection. Graph analysis corresponding to CP with and without LPS injection supports the observation above described, meaning that CP injected with LPS had a significant increase ($p \leq 0.01$) of CD11b fluorescence intensity when compared to control. This increase in CD11b expression is verified at both ages (1 and 3 months) (Figure 48).

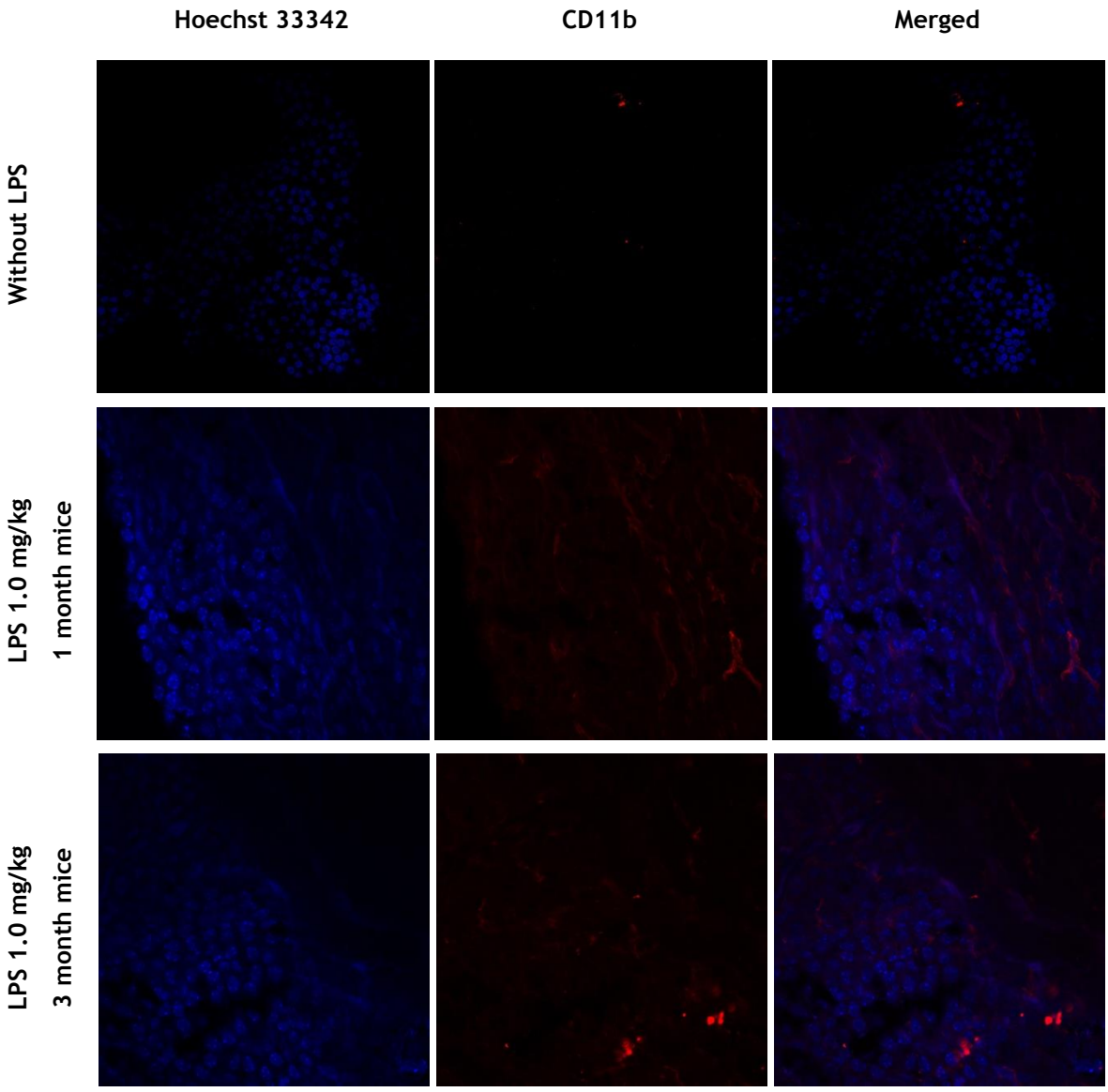

Figure 47: Representative confocal images of LPS effects on CP CD11b expression. Image represent CD11B expression in CP explants 28 days after 1.0 mg/kg of LPS intraperitoneal administration in 1 and 3 month mice. LPS-lipopolysaccharide

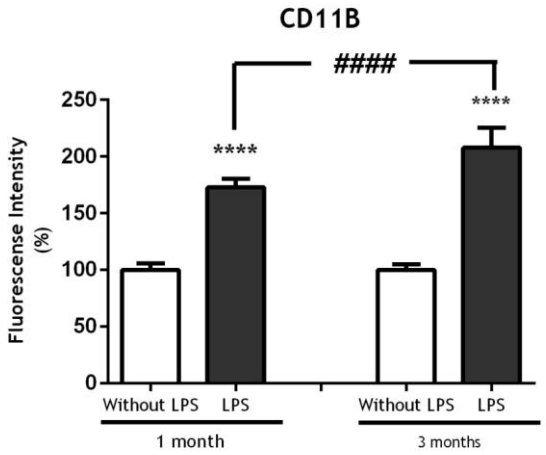

Figure 48: Effect of LPS in CP *in vivo* CD11b expression. Comparison of CD11b levels through measurement of mean fluorescence intensity in CP explants from 1 month and 3 months mice injected with 1.0 mg/kg of LPS or without LPS. Data show mean values ±SEM from experiments with n=4. Statistical analysis was performed using the ANOVA. LPS vs. without LPS (****P≤0.0001); 1 month vs. 3 months(####P≤0.0001). LPS- lipopolysaccharide.

4.4.3 NeuN

It was not possible to have a conclusive result about alterations in NeuN expression after LPS injection. However, after fluorescence analysis we observed a significant decrease ($p \leq 0.05$) in NeuN expression 28 days after LPS injection (Figure 50). This reduction in NeuN expression was verified at both ages studied (1 and 3 month).

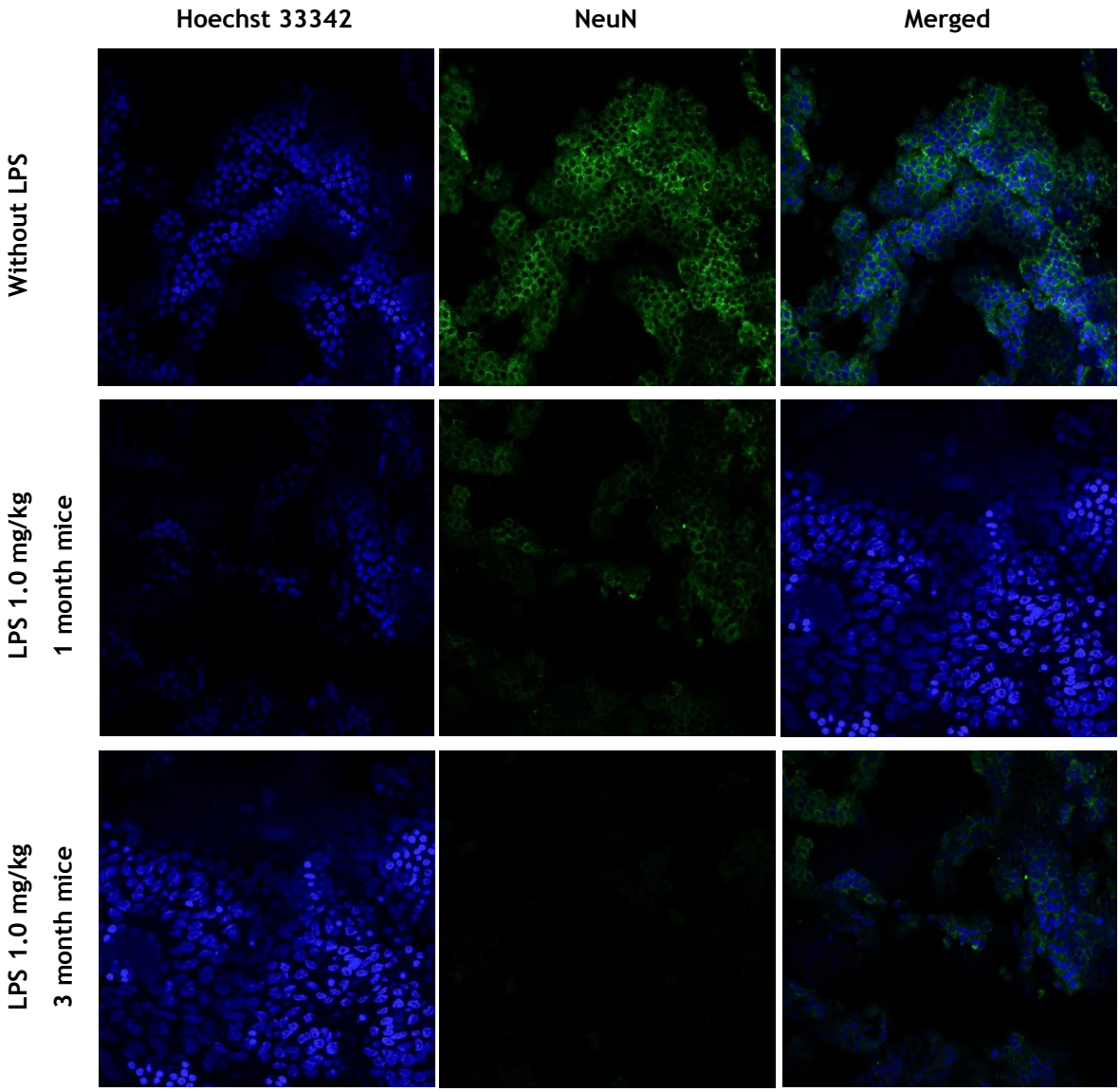

Figure 49: Representative confocal images of LPS effects on CP NeuN expression. Image represent NeuN expression in CP explants 28 days after 1.0 mg/kg of LPS intraperitoneal administration in 1 and 3 month mice. LPS-lipopolysaccharide; NeuN- Neuronal Nuclear Protein.

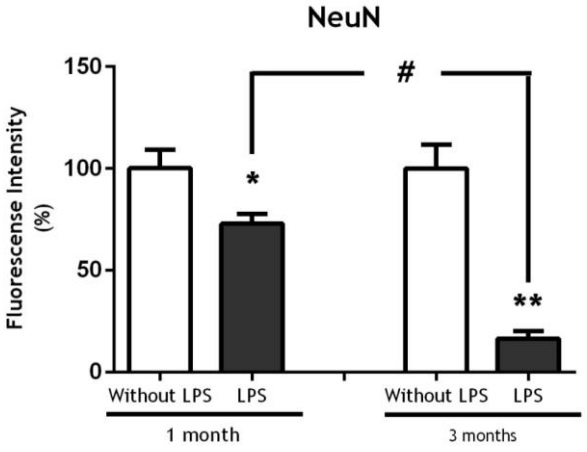

Figure 50: Effect of LPS in CP *in vivo* NeuN expression. Comparison of NeuN levels through measurement of mean fluorescence intensity in CP explants from 1 month and 3 months mice injected with 1.0 mg/kg of LPS or without LPS. Data show mean values ±SEM from experiments with n=4. Statistical analysis was performed using the ANOVA. LPS vs. without LPS (*P≤0.05 and **P≤0.01); 1 month vs. 3 months(#P≤0.01). LPS- lipopolysaccharide. NeuN- Neuronal Nuclear Protein.

4.4.4 GFAP

Observing figure 51, it is possible to report that a change in GFAP expression occurs 28 days after LPS injection. The observation of the graph corresponding to CP with and without LPS injection supports the observation above described, meaning that CP injected with LPS had a significant increase ($p \leq 0.01$) in fluorescence intensity of GFAP when compared to control. This increase in GFAP expression is verified at 1 and 3 months (Figure 52).

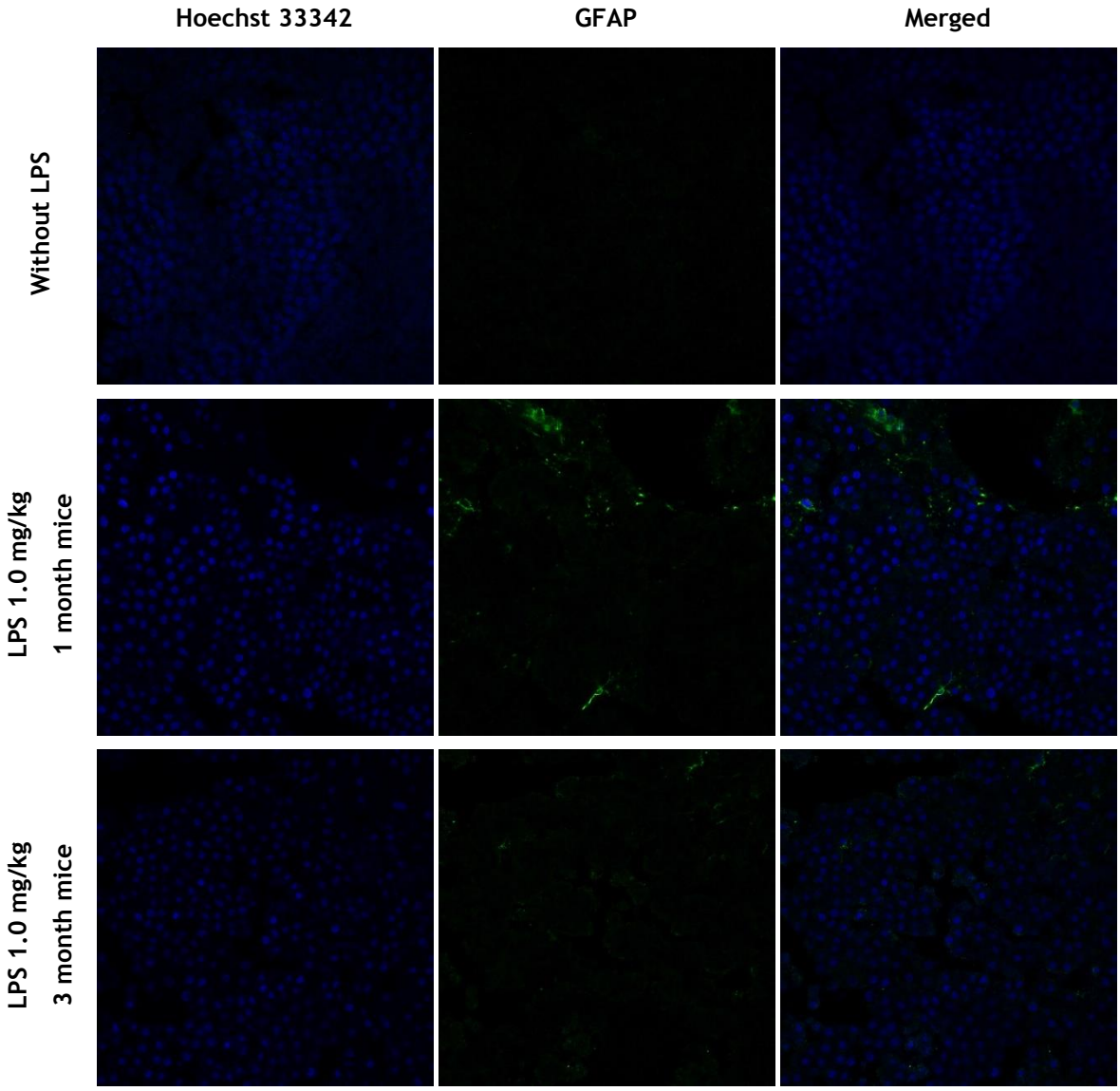

Figure 51: Representative confocal images of LPS effects on CP GFAP expression. Image represent GFAP expression in CP explants 28 days after 1.0 mg/kg of LPS intraperitoneal administration in 1 and 3 month mice. LPS-lipopolysaccharide, GFAP- Glial Fibrillary Acidic Protein.

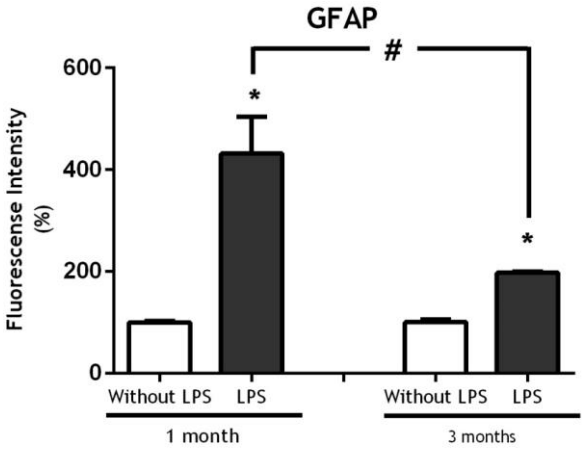

Figure 52: Effect of LPS in CP *in vivo* GFAP expression. Comparison of GFAP levels through measurement of mean fluorescence intensity in CP explants from 1 month and 3 months mice injected with 1.0 mg/kg of LPS or without LPS. Data show mean values ±SEM from experiments with n=4. Statistical analysis was performed using the ANOVA. LPS vs. without LPS (*P≤0.05); 1 month vs. 3 months(#P≤0.05). LPS- lipopolysaccharide ; GFAP- Glial Fibrillary Acidic Protein.

Chapter 5. Discussion and Conclusion

5. Discussion and conclusion

The BCSFB represents an important barrier and simultaneously, a route of communication between the periphery and the CNS. The CP is ideally located to respond to peripheral stimulus, since it is well vascularized by fenestrated capillaries and because it produces most of the CSF (65). An altered profile of proteins secreted into the CSF may affect CNS function in health and disease. Many of such disorders, including AD and PD, are known to have an underlying inflammatory component. Thus, a specific study on the profile of CP secreted proteins during inflammation may provide key information for physiological and pathological conditions.

Thus, the aim of this work was to evaluate the effect of a neuroinflammatory insult to the neurogenic potential, protein synthesis, oxidative stress and barrier function of the CP.

The study of oxidative stress in CP after a neuroinflammatory insult was analyzed *in vitro*, *ex vivo* and *in vivo*. The production of ROS and NO was measured in CPEC after an insult with LPS, and *ex vivo* using CP of newborn rats and 21 days rats for ROS and iNOS quantification. iNOS quantification was carried out *in vivo* in 1, 3 and 9 months mice.

Small molecule mediators, such as NO and ROS, have well-described roles in inflammatory processes in various tissues (30, 66). During neuroinflammation, iNOS is expressed by neurons and glial cells in response to pro-inflammatory cytokines (30). In this study, an increase of oxidative stress in CPEC and CP explants of newborn and 21 days rats was observed. Release of ROS and NO occurred immediately after the CPEC exposure to the inflammatory agent LPS, and had a peak of production approximately 2 hours after stimulus for the two reactive species (Figure 9 and 10). Considering the ROS results obtained in CP *in vitro*, we conducted ROS detection *ex vivo* using the DCFH-DA method. This experiment was carried out in CP of newborn and 21 days rats, incubated with LPS during two hours and subsequently incubated with DCFH-DA that emits green fluorescence when connected to free radicals. A ROS increase was detected in both ages (Figure 23), but this effect was nearly 5 times more pronounced in 21 day-old animals. Studies correlating ROS production with age report an increase in the imbalance of the normal redox state that exponentially increases with age, paralleled by a remarkable decline of the cell repair machinery (67). These findings support the difference in ROS production observed in our study among ages, although 21 days rats can be considered young animals. *Ex vivo* and *in vivo* studies were performed to further analyze the production of iNOS by Western blot in 21 days rats, *ex vivo*, and in 1, 3 and 9 months mice, *in vivo*. Untreated CP explants or CP explants from animal injected with vehicle, did not express iNOS and that the ones injected or incubated with LPS expressed it (Figure 41). *Ex vivo*, we

observed a significantly difference between CP explants incubated with LPS compared to control. *In vivo*, it was only possible to perform two assays, so it was not possible to assert a conclusion, concerning the statistical significance.

Microglia has two main functions within the CNS: maintenance of neuronal functions and immune defense. However, deregulated and/or sustained activation of microglia may induce neuroinflammation and contribute to progression of almost all brain diseases (68, 69). Our results propose that CP is involved in microglia activation, due to the significant increase in CD11b expression, a microglial marker, in CP explants from newborns and 21 days rats after 48 hours of incubation with 0.1 µg/mL of LPS, when compared to untreated controls. After observing the effect of LPS in CP, we proposed to study the alterations of microglial activation with age. The effects of aging on neuroinflammation of CP were analyzed in explants of newborn and 21 days rats, which were incubated with 0.1µg/mL LPS for 48 hours.
Regarding the study of neuroinflammation, a significant increase of CD11b labeling in newborn and 21 days rats CP was verified; however, in newborn rats the increase was approximately 7 times more pronounced higher than in 21 days rats (Figure 27).
The effect of LPS was evaluated *in vivo* to complement the *ex vivo* study. The same results were observed in CP obtained from 1 and 3 months mice, 28 days after injection with LPS, when compared to controls. Interestingly, in vivo, in older rats (3 months) activation of microglia was higher when compared to 1 month rats (72% versus 107%, respectively) (Figure 47).

CP is the major local of TTR production, a protein described to be altered in ND and involved in neuroinflammatory processes like AD and PD (2, 70, 71). Considering this, TTR was quantified in the extracellular medium of CPEC at different incubation times (1, 2, 4, 6, 8, 12, 18 and 24 hours) with and without LPS. Surprisingly, after 1 hour of incubation, CPEC had increased more than 50% the release of TTR to the medium. (14). To observe if TTR expression in CP explants and *in vivo* were altered with neuroinflammatory insult, several experiments were performed. The results of the different experiments did not show changes in TTR expression between LPS treated and controls in the different experimental setups. However, in explants of mice injected with 1.0 mg/kg of LPS, performed by WB in 1,3 and 9 month mice, TTR synthesis decreased with age, with a significant reduction between 1 and 9 months mice. A scientific support for this fact is related to protein synthesis(72), particularly TTR (73), counts down along age in CP.

The TJ participate in two major functions in the cell: a barrier function, namely regulating the permeability of solutes between adjacent cells; and a fence function, controlling the lateral diffusion of proteins within the lipid bilayer (74). TJ confers to BBB the capacity to preclude blood substance from permeating. Considering the importance of BCSFB, we studied the morphologic and expression alterations of TJ, using CPEC as model, in a

neuroinflammatory environment. In many experimental neuronal disease models, TJ-related proteins like ZO-1, occludin and E-cadherin proved to be reduced (19, 24, 26) compared with healthy animals. In neuroinflammatory response, BBB integrity is compromised, leading to the leakage of blood cells, which further aggravate inflammation and generate neurotoxic products that can finally result in neuron death (75). In this study, we observed a decreased expression of TJ proteins in the LPS-treated group versus the control group, in CPEC, through immunofluorescence quantification of occludin and ZO-1, which revealed a significant decrease. Nonetheless, claudin-1 and E-cadherin, levels remained unaffected. We did observe an alteration in distribution and morphology of TJ. *Ex vivo* results confirmed no differences in E-cadherin expression in CP explants incubated with LPS when compared to untreated CP explants. The study of occludin expression *ex vivo* demonstrated that it remained unchanged, in contrast with CPEC immunofluorescence assays, where a reduction of this protein expression was observed. In vivo, in mice injected with 1.0 mg/kg of LPS at 1, 3 and 9 months we found that E-cadherin and occludin expression decreased with age, indicating a decrease in CP capacity as barrier along ageing. However, it was not possible to confirm these results, as this experiment had only two replicates. Our results was in accordance to with obtain by Krouwer *et al.*, 2012 (76) Our results demonstrated that, morphologically, CPEC keep their integrity since proteins that encode TJ are expressed on it, but the alteration in TJ proteins expression after LPS insults indicates that a disturbance occurred and consequently, CP functions might be compromised.

Several studies described that neuroinflammation is reflected in AD and PD as astrogliosis and microglial activation (2, 70, 71). Reactive astrocytes may play a critical role in sustaining this neuroinflammatory response following systemic LPS injection in mouse, as well as other neuro-immune cell types (77, 78). Also, previous reports stated that CPEC have the capacity to proliferate and differentiate into other type of cells (79, 80), based on the existence of a subpopulation of neural progenitor cells within the CP (81). The proliferation of CPEC was reported in an experimental model of ischemic brain injury in rats where cells in the CP expressed GFAP and NeuN (68).

Our present findings suggest that neuroinflammation regulates the proliferation and differentiation of neural progenitor cells in the CP, with an increase in GFAP after 48 hours of CP incubation with 0.1 µg/mL of LPS, when compared to untreated controls. The same trend was observed in mice injected once with 1.0 mg/kg of LPS. However, NeuN (neuron marker) expression decreased significantly in *ex vivo* assays after incubation with 0.1 µg/mL of LPS and similarly, this decline was observed on *in vivo* studies in mice with 1 and 3 months, 28 days after LPS injection. Together, these results converge with those present by Carro *et al.*, 2013 (79), that described that NeuN positive cells decrease when amyloidogenic environment occurs, supporting the already described effect that neuroinflammation down-regulate neurogenesis.

The literature refers that the differentiation of cells decreases with age, in different tissues, particularly in the hippocampus and olfactory bulbs (77). The effects of aging on neurogenesis of CP were analyzed in explants of newborn and 21 days rats, which were incubated with 0.1µg/mL LPS for 48 hours. The results concerning NeuN expression demonstrated a reduction for both newborn and 21 days animals, showing a significant difference between them, with a diminution in NeuN expression of 75% and 25%, respectively, when compared with controls (Figure 29). The analysis of GFAP labeling, an astrocytes marker, in CP explants, revealed no significant changes between the two age groups studied, the same results was verified in hippocampus by Fu *et al.*, 2014 (77) (Figure 31).

In order to expand our model of study, the effect of LPS was evaluated *in vivo* with an extended study to animals with 1 and 3 months, injected with 1.0 mg/kg of LPS and sacrificed 28 days after. Regarding neurogenesis and astrogliosis, a decrease was observed. In explants from mice with 1 month a decrease of 26% in NeuN was observed against 83.87% in 3 months mice, but for GFAP we observed an augment of 234% between the two age groups, being the higher increase detected in animals with 1 month. Our results prove that adult neurogenesis is ongoing and assumed to continue throughout the entire lifespan of an animal. Several studies, have demonstrated that neural stem-cell proliferation decreases with age (82-84).

In summary, the neuroinflammatory process induced by LPS, led to a decrease in neurogenesis and an increase in microglia activation, astrogliosis, iNOS expression, and ROS and NO production, as well as decrease in the barrier function that will cause CP dysfunctions and chronic brain inflammation. In other hand, a health CP promotes neurogenesis and a decrease of microglia activation and astrogliosis, which allows maintenance of CP homeostasis (Figure 53).

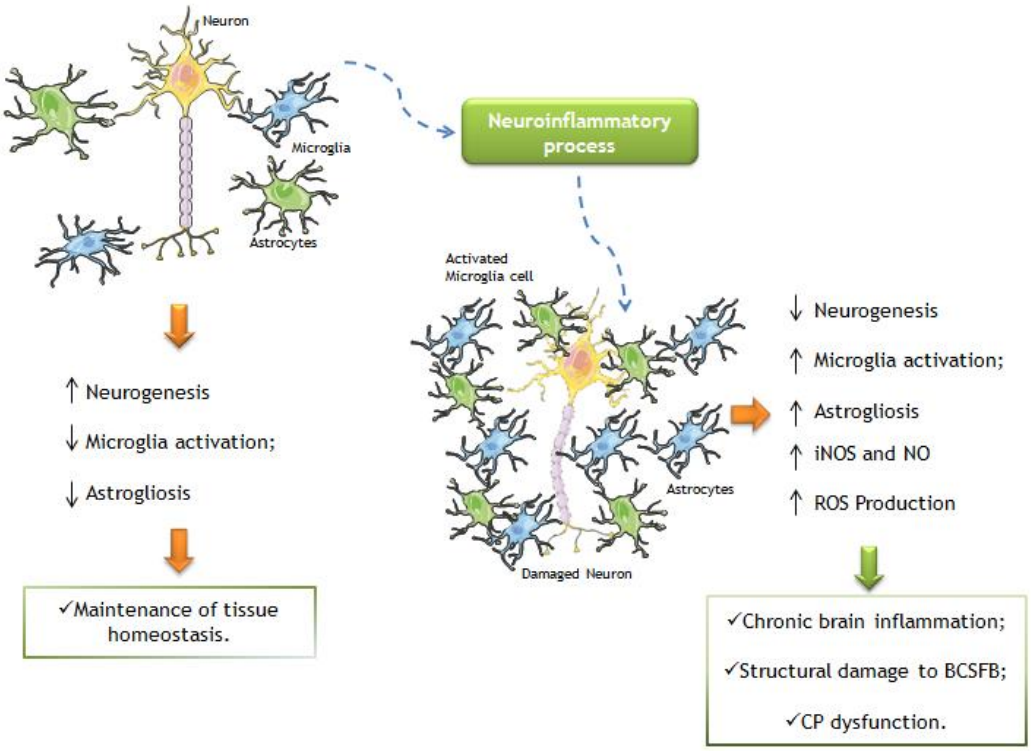

Figure 53: Effect of LPS in CP. Resume of the response to neuroinflammation CP *in vitro*, *ex vivo* and *in vivo*, through the LPS insult, an endotoxin capable of inducing inflammation.

Chapter 6. Future perspectives

6. Future perspectives

In this study, we observed that CP responds to neuroinflammation induced by LPS. Previous studies by our working group found that sexual hormones interfered positively in AD. In the future, it would be pertinent investigate sexual hormones effects in CP on the observed results, i.e., activation of microglia, decreased neurogenesis, oxidative stress and disruption of BCSFB. In this way, pre and/or post-treatment of CP with sexual hormones, as estradiol or testosterone, could be performed. Later, if appropriate, pathways and mechanisms underlying should be verified. For example, through blocking estrogen receptor via in way to verify the involvement of the route of action of estrogens. Thus, considering the results and protocols optimized during this study, it would be interesting, in a first approach, to see if sexual hormones, would take effects in CPEC, in the neuroinflammatory markers studied. Depending of results, posteriorly, the study in CPEC might be extrapolated to *ex vivo* and *in vivo* studies.

It would be also pertinent to check if CP recovers over time after a LPS insult. To analyze this hypothesis, animals may be injected at a particular time and sacrificed at different times after. Then, evaluation of the neuroinflammatory and neurogenic markers would be carried out.

Finally, taken into account several studies that describe that neuroinflammation leads to Aß aggregation (85, 86), in different structures of the brain; it would be interesting to observe if this aggregation occurs in the CP. If so, the study of sex hormones effect on it should be study.

7. References

1. Marieb EN, Hoehn K. Anatomy and Physiology: Pearson Benjamin Cummings; 2008.

2. Hsieh HL, Yang CM. Role of redox signaling in neuroinflammation and neurodegenerative diseases. BioMed research international. 2013;2013:484613. Epub 2014/01/24.

3. Steele ML, Robinson SR. Reactive astrocytes give neurons less support: implications for Alzheimer's disease. Neurobiol Aging. 2012;33(2):3.

4. Gimsa U, Mitchison NA, Brunner-Weinzierl MC. Immune privilege as an intrinsic CNS property: astrocytes protect the CNS against T-cell-mediated neuroinflammation. Mediators of inflammation. 2013;2013:320519. Epub 2013/09/12.

5. Damkier HH, Brown PD, Praetorius J. Epithelial pathways in choroid plexus electrolyte transport. Physiology. 2010;25(4):239-49.

6. Wolburg H, Paulus W. Choroid plexus: biology and pathology. Acta neuropathologica. 2010;119(1):75-88. Epub 2009/12/25.

7. Quintelas C, Pereira R, Kaplan E, Tavares T. Removal of Ni(II) from aqueous solutions by an Arthrobacter viscosus biofilm supported on zeolite: from laboratory to pilot scale. Bioresource technology. 2013;142:368-74. Epub 2013/06/12.

8. Damkier HH, Brown PD, Praetorius J. Cerebrospinal fluid secretion by the choroid plexus. Physiological reviews. 2013;93(4):1847-92. Epub 2013/10/19.

9. Marques F, Sousa JC, Coppola G, Gao F, Puga R, Brentani H, et al. Transcriptome signature of the adult mouse choroid plexus. Fluids and barriers of the CNS. 2011;8(1):10. Epub 2011/02/26.

10. Mortazavi MM, Griessenauer CJ, Adeeb N, Deep A, Bavarsad Shahripour R, Loukas M, et al. The choroid plexus: a comprehensive review of its history, anatomy, function, histology, embryology, and surgical considerations. Child's nervous system : ChNS : official journal of the International Society for Pediatric Neurosurgery. 2014;30(2):205-14. Epub 2013/11/30.

11. Serot JM, Bene MC, Faure GC. Choroid plexus, aging of the brain, and Alzheimer's disease. Front Biosci. 2003;1(8):s515-21.

12. Emerich DF, Vasconcellos AV, Elliott RB, Skinner SJ, Borlongan CV. The choroid plexus: function, pathology and therapeutic potential of its transplantation. Expert opinion on biological therapy. 2004;4(8):1191-201. Epub 2004/07/23.

13. Zappaterra MW, Lehtinen MK. The cerebrospinal fluid: regulator of neurogenesis, behavior, and beyond. Cellular and molecular life sciences : CMLS. 2012;69(17):2863-78. Epub 2012/03/15.

14. Martinho A, Goncalves I, Santos CR. Glucocorticoids regulate metallothionein-1/2 expression in rat choroid plexus: effects on apoptosis. Molecular and cellular biochemistry. 2013;376(1-2):41-51. Epub 2013/01/08.

15. Spuch C, Carro E. The p75 neurotrophin receptor localization in blood-CSF barrier: expression in choroid plexus epithelium. BMC neuroscience. 2011;12:39. Epub 2011/05/17.

16. Schroten M, Hanisch FG, Quednau N, Stump C, Riebe R, Lenk M, et al. A novel porcine in vitro model of the blood-cerebrospinal fluid barrier with strong barrier function. PloS one. 2012;7(6):e39835. Epub 2012/06/30.

17. Goncalves A, Ambrosio AF, Fernandes R. Regulation of claudins in blood-tissue barriers under physiological and pathological states. Tissue barriers. 2013;1(3):e24782. Epub 2014/03/26.

18. Bednarczyk J, Lukasiuk K. Tight junctions in neurological diseases. Acta neurobiologiae experimentalis. 2011;71(4):393-408. Epub 2012/01/13.

19. Stolp HB, Liddelow SA, Sa-Pereira I, Dziegielewska KM, Saunders NR. Immune responses at brain barriers and implications for brain development and neurological function in later life. Frontiers in integrative neuroscience. 2013;7:61. Epub 2013/08/30.

20. Szmydynger-Chodobska J, Pascale CL, Pfeffer AN, Coulter C, Chodobski A. Expression of junctional proteins in choroid plexus epithelial cell lines: a comparative study. Cerebrospinal fluid research. 2007;4:11. Epub 2007/12/29.

21. Liu WY, Wang ZB, Zhang LC, Wei X, Li L. Tight junction in blood-brain barrier: an overview of structure, regulation, and regulator substances. CNS neuroscience & therapeutics. 2012;18(8):609-15. Epub 2012/06/13.

22. Runkle EA, Mu D. Tight junction proteins: from barrier to tumorigenesis. Cancer letters. 2013;337(1):41-8. Epub 2013/06/08.

23. Aijaz S, Balda MS, Matter K. Tight junctions: molecular architecture and function. Int Rev Cytol. 2006;248:261-98.

24. Wolburg H, Wolburg-Buchholz K, Liebner S, Engelhardt B. Claudin-1, claudin-2 and claudin-11 are present in tight junctions of choroid plexus epithelium of the mouse. Neurosci Lett. 2001;307(2):77-80.

25. Itoh M, Nagafuchi A, Yonemura S, Kitani-Yasuda T, Tsukita S. The 220-kD protein colocalizing with cadherins in non-epithelial cells is identical to ZO-1, a tight junction-associated protein in epithelial cells: cDNA cloning and immunoelectron microscopy. J Cell Biol. 1993;121(3):491-502.

26. Lanz TV, Becker S, Osswald M, Bittner S, Schuhmann MK, Opitz CA, et al. Protein kinase Cbeta as a therapeutic target stabilizing blood-brain barrier disruption in experimental autoimmune encephalomyelitis. Proceedings of the National Academy of Sciences of the United States of America. 2013;110(36):14735-40. Epub 2013/08/21.

27. Marques F, Sousa JC, Coppola G, Geschwind DH, Sousa N, Palha JA, et al. The choroid plexus response to a repeated peripheral inflammatory stimulus. BMC neuroscience. 2009;10:135. Epub 2009/11/20.

28. Ling GS, Bennett J, Woollard KJ, Szajna M, Fossati-Jimack L, Taylor PR, et al. Integrin CD11b positively regulates TLR4-induced signalling pathways in dendritic cells but not in macrophages. Nature communications. 2014;5:3039. Epub 2014/01/16.

29. Skripuletz T, Miller E, Grote L, Gudi V, Pul R, Voss E, et al. Lipopolysaccharide delays demyelination and promotes oligodendrocyte precursor proliferation in the central nervous system. Brain, behavior, and immunity. 2011;25(8):1592-606. Epub 2011/06/04.

30. Heneka MT, Kummer MP, Latz E. Innate immune activation in neurodegenerative disease. Nature reviews Immunology. 2014;14(7):463-77. Epub 2014/06/26.

31. Song JH, Lee JW, Shim B, Lee CY, Choi S, Kang C, et al. Glycyrrhizin alleviates neuroinflammation and memory deficit induced by systemic lipopolysaccharide treatment in mice. Molecules. 2013;18(12):15788-803. Epub 2013/12/20.

32. Amor S, Peferoen LA, Vogel DY, Breur M, van der Valk P, Baker D, et al. Inflammation in neurodegenerative diseases - an update. Immunology. 2013;16(10):12233.

33. Skaper SD, Giusti P, Facci L. Microglia and mast cells: two tracks on the road to neuroinflammation. Faseb J. 2012;26(8):3103-17.

34. Ransohoff RM, Brown MA. Innate immunity in the central nervous system. J Clin Invest. 2012;122(4):1164-71.

35. Schwartz M, Baruch K. The resolution of neuroinflammation in neurodegeneration: leukocyte recruitment via the choroid plexus. The EMBO journal. 2014;33(1):7-22. Epub 2013/12/21.

36. Rahal A, Kumar A, Singh V, Yadav B, Tiwari R, Chakraborty S, et al. Oxidative stress, prooxidants, and antioxidants: the interplay. BioMed research international. 2014;2014:761264. Epub 2014/03/04.

37. Dickinson AC, DeJordy JO, Boutin MG, Teres D. Absence of generation of oxygen-containing free radicals with 4'-deoxydoxorubicin, a non-cardiotoxic anthracycline drug. Biochem Biophys Res Commun. 1984;125(2):584-91.

38. Miyamoto M, Hashimoto K, Minagawa K, Satoh K, Komatsu N, Fujimaki M, et al. Effect of poly-herbal formula on NO production by LPS-stimulated mouse macrophage-like cells. Anticancer Res. 2002;22(6A):3293-301.

39. Pavanato A, Tunon MJ, Sanchez-Campos S, Marroni CA, Llesuy S, Gonzalez-Gallego J, et al. Effects of quercetin on liver damage in rats with carbon tetrachloride-induced cirrhosis. Dig Dis Sci. 2003;48(4):824-9.

40. Shechter R, Miller O, Yovel G, Rosenzweig N, London A, Ruckh J, et al. Recruitment of beneficial M2 macrophages to injured spinal cord is orchestrated by remote brain choroid plexus. Immunity. 2013;38(3):555-69. Epub 2013/03/13.

41. Quintela T, Goncalves I, Martinho A, Alves CH, Saraiva MJ, Rocha P, et al. Progesterone enhances transthyretin expression in the rat choroid plexus in vitro and in vivo via progesterone receptor. Journal of molecular neuroscience : MN. 2011;44(3):152-8. Epub 2010/06/11.

42. Martinho A, Santos CR, Goncalves I. A distal estrogen responsive element upstream the cap site of human transthyretin gene is an enhancer-like element upon ERalpha and/or ERbeta transactivation. Gene. 2013;527(2):469-76. Epub 2013/07/19.

43. Martinho A, Goncalves I, Cardoso I, Almeida MR, Quintela T, Saraiva MJ, et al. Human metallothioneins 2 and 3 differentially affect amyloid-beta binding by transthyretin. The FEBS journal. 2010;277(16):3427-36. Epub 2010/07/22.

44. Sousa JC, Grandela C, Fernandez-Ruiz J, de Miguel R, de Sousa L, Magalhaes AI, et al. Transthyretin is involved in depression-like behaviour and exploratory activity. J Neurochem. 2004;88(5):1052-8.

45. Cascella R, Conti S, Mannini B, Li X, Buxbaum JN, Tiribilli B, et al. Transthyretin suppresses the toxicity of oligomers formed by misfolded proteins in vitro. Biochim Biophys Acta. 2013;1832(12):2302-14. Epub 2013/10/01.

46. Gilbert BJ. The role of amyloid beta in the pathogenesis of Alzheimer's disease. Journal of clinical pathology. 2013;66(5):362-6. Epub 2013/03/26.

47. Liu CC, Kanekiyo T, Xu H, Bu G. Apolipoprotein E and Alzheimer disease: risk, mechanisms and therapy. Nature reviews Neurology. 2013;9(2):106-18. Epub 2013/01/09.

48. Zlokovic BV. Neurovascular pathways to neurodegeneration in Alzheimer's disease and other disorders. Nature reviews Neuroscience. 2011;12(12):723-38. Epub 2011/11/04.

49. Warren JD, Fletcher PD, Golden HL. The paradox of syndromic diversity in Alzheimer disease. Nature reviews Neurology. 2012;8(8):451-64. Epub 2012/07/18.

50. Ittner LM, Gotz J. Amyloid-beta and tau--a toxic pas de deux in Alzheimer's disease. Nature reviews Neuroscience. 2011;12(2):65-72. Epub 2011/01/05.

51. Nie Q, Du XG, Geng MY. Small molecule inhibitors of amyloid beta peptide aggregation as a potential therapeutic strategy for Alzheimer's disease. Acta pharmacologica Sinica. 2011;32(5):545-51. Epub 2011/04/19.

52. Krzyzanowska A, Carro E. Pathological alteration in the choroid plexus of Alzheimer's disease: implication for new therapy approaches. Frontiers in pharmacology. 2012;3:75. Epub 2012/05/09.

53. Irwin DJ, Lee VM, Trojanowski JQ. Parkinson's disease dementia: convergence of alpha-synuclein, tau and amyloid-beta pathologies. Nature reviews Neuroscience. 2013;14(9):626-36. Epub 2013/08/01.

54. Nolan YM, Sullivan AM, Toulouse A. Parkinson's disease in the nuclear age of neuroinflammation. Trends in molecular medicine. 2013;19(3):187-96. Epub 2013/01/16.

55. More SV, Kumar H, Kim IS, Song SY, Choi DK. Cellular and molecular mediators of neuroinflammation in the pathogenesis of Parkinson's disease. Mediators of inflammation. 2013;2013:952375. Epub 2013/08/13.

56. Kohman RA, Rhodes JS. Neurogenesis, inflammation and behavior. Brain, behavior, and immunity. 2013;27(1):22-32. Epub 2012/09/19.

57. Taupin P. BrdU immunohistochemistry for studying adult neurogenesis: paradigms, pitfalls, limitations, and validation. Brain research reviews. 2007;53(1):198-214. Epub 2006/10/06.

58. Iascone DM, Padidam S, Pyfer MS, Zhang X, Zhao L, Chin J. Impairments in neurogenesis are not tightly linked to depressive behavior in a transgenic mouse model of Alzheimer's disease. PloS one. 2013;8(11):e79651. Epub 2013/11/19.

59. Fuster-Matanzo A, Llorens-Martin M, Hernandez F, Avila J. Role of neuroinflammation in adult neurogenesis and Alzheimer disease: therapeutic approaches. Mediators of inflammation. 2013;2013:260925. Epub 2013/05/22.

60. Monje ML, Palmer T. Radiation injury and neurogenesis. Curr Opin Neurol. 2003;16(2):129-34.

61. Gomes A, Fernandes E, Lima JL. Fluorescence probes used for detection of reactive oxygen species. Journal of biochemical and biophysical methods. 2005;65(2-3):45-80. Epub 2005/11/22.

62. Cristovao AC, Saavedra A, Fonseca CP, Campos F, Duarte EP, Baltazar G. Microglia of rat ventral midbrain recovers its resting state over time in vitro: let microglia rest before work. Journal of neuroscience research. 2010;88(3):552-62. Epub 2009/09/10.

63. Clauzure M, Valdivieso AG, Massip Copiz MM, Schulman G, Teiber ML, Santa-Coloma TA. Disruption of Interleukin-1beta Autocrine Signaling Rescues Complex I Activity and Improves ROS Levels in Immortalized Epithelial Cells with Impaired Cystic Fibrosis Transmembrane Conductance Regulator (CFTR) Function. PloS one. 2014;9(6):e99257. Epub 2014/06/06.

64. Johanson C, Stopa E, McMillan P, Roth D, Funk J, Krinke G. The distributional nexus of choroid plexus to cerebrospinal fluid, ependyma and brain: toxicologic/pathologic phenomena, periventricular destabilization, and lesion spread. Toxicologic pathology. 2011;39(1):186-212. Epub 2010/12/30.

65. Matsumoto J, Takata F, Machida T, Takahashi H, Soejima Y, Funakoshi M, et al. Tumor necrosis factor-alpha-stimulated brain pericytes possess a unique cytokine and chemokine release profile and enhance microglial activation. Neurosci Lett. 2014;578:133-8. Epub 2014/07/06.

66. Lucas K, Maes M. Role of the Toll Like receptor (TLR) radical cycle in chronic inflammation: possible treatments targeting the TLR4 pathway. Molecular neurobiology. 2013;48(1):190-204. Epub 2013/02/26.

67. Cencioni C, Spallotta F, Martelli F, Valente S, Mai A, Zeiher AM, et al. Oxidative stress and epigenetic regulation in ageing and age-related diseases. International journal of molecular sciences. 2013;14(9):17643-63. Epub 2013/08/31.

68. Cazareth J, Guyon A, Heurteaux C, Chabry J, Petit-Paitel A. Molecular and cellular neuroinflammatory status of mouse brain after systemic lipopolysaccharide challenge: importance of CCR2/CCL2 signaling. Journal of neuroinflammation. 2014;11(1):132. Epub 2014/07/30.

69. Liu Y, Zhang R, Yan K, Chen F, Huang W, Lv B, et al. Mesenchymal stem cells inhibit lipopolysaccharide-induced inflammatory responses of BV2 microglial cells through TSG-6. Journal of neuroinflammation. 2014;11:135. Epub 2014/08/05.

70. Corraliza I. Recruiting specialized macrophages across the borders to restore brain functions. Frontiers in cellular neuroscience. 2014;8:262. Epub 2014/09/18.

71. Takeuchi H, Suzumura A. Gap junctions and hemichannels composed of connexins: potential therapeutic targets for neurodegenerative diseases. Frontiers in cellular neuroscience. 2014;8:189. Epub 2014/09/18.

72. Johanson CE, Stopa EG, McMillan PN. The blood-cerebrospinal fluid barrier: structure and functional significance. Methods Mol Biol. 2011;686:101-31. Epub 2010/11/18.

73. Chen RL, Athauda SB, Kassem NA, Zhang Y, Segal MB, Preston JE. Decrease of transthyretin synthesis at the blood-cerebrospinal fluid barrier of old sheep. J Gerontol A Biol Sci Med Sci. 2005;60(7):852-8.

74. Winger RC, Koblinski JE, Kanda T, Ransohoff RM, Muller WA. Rapid Remodeling of Tight Junctions during Paracellular Diapedesis in a Human Model of the Blood-Brain Barrier. J Immunol. 2014;193(5):2427-37. Epub 2014/07/27.

75. Liu T, Zhang T, Yu H, Shen H, Xia W. Adjudin protects against cerebral ischemia reperfusion injury by inhibition of neuroinflammation and blood-brain barrier disruption. Journal of neuroinflammation. 2014;11:107. Epub 2014/06/15.

76. Krouwer VJ, Hekking LH, Langelaar-Makkinje M, Regan-Klapisz E, Post JA. Endothelial cell senescence is associated with disrupted cell-cell junctions and increased monolayer permeability. Vascular cell. 2012;4(1):12. Epub 2012/08/30.

77. Fu HQ, Yang T, Xiao W, Fan L, Wu Y, Terrando N, et al. Prolonged neuroinflammation after lipopolysaccharide exposure in aged rats. PloS one. 2014;9(8):e106331. Epub 2014/08/30.

78. Brenner M. Role of GFAP in CNS injuries. Neurosci Lett. 2014;565C:7-13. Epub 2014/02/11.

79. Bolos M, Spuch C, Ordonez-Gutierrez L, Wandosell F, Ferrer I, Carro E. Neurogenic effects of beta-amyloid in the choroid plexus epithelial cells in Alzheimer's disease. Cellular and molecular life sciences : CMLS. 2013;70(15):2787-97. Epub 2013/03/05.

80. Emerich DF, Skinner SJ, Borlongan CV, Thanos CG. A role of the choroid plexus in transplantation therapy. Cell transplantation. 2005;14(10):715-25. Epub 2006/02/04.

81. Itokazu Y, Kitada M, Dezawa M, Mizoguchi A, Matsumoto N, Shimizu A, et al. Choroid plexus ependymal cells host neural progenitor cells in the rat. Glia. 2006;53(1):32-42. Epub 2005/09/15.

82. Larson TA, Thatra NM, Lee BH, Brenowitz EA. Reactive neurogenesis in response to naturally occurring apoptosis in an adult brain. The Journal of neuroscience : the official journal of the Society for Neuroscience. 2014;34(39):13066-76. Epub 2014/09/26.

83. Leuner B, Kozorovitskiy Y, Gross CG, Gould E. Diminished adult neurogenesis in the marmoset brain precedes old age. Proceedings of the National Academy of Sciences of the United States of America. 2007;104(43):17169-73. Epub 2007/10/18.

84. Wang N, Hurley P, Pytte C, Kirn JR. Vocal control neuron incorporation decreases with age in the adult zebra finch. The Journal of neuroscience : the official journal of the Society for Neuroscience. 2002;22(24):10864-70. Epub 2002/12/18.

85. Jacobs AH, Tavitian B. Noninvasive molecular imaging of neuroinflammation. Journal of cerebral blood flow and metabolism : official journal of the International Society of Cerebral Blood Flow and Metabolism. 2012;32(7):1393-415. Epub 2012/05/03.

86. Amor S, Puentes F, Baker D, van der Valk P. Inflammation in neurodegenerative diseases. Immunology. 2010;129(2):154-69. Epub 2010/06/22.

8. Appendix

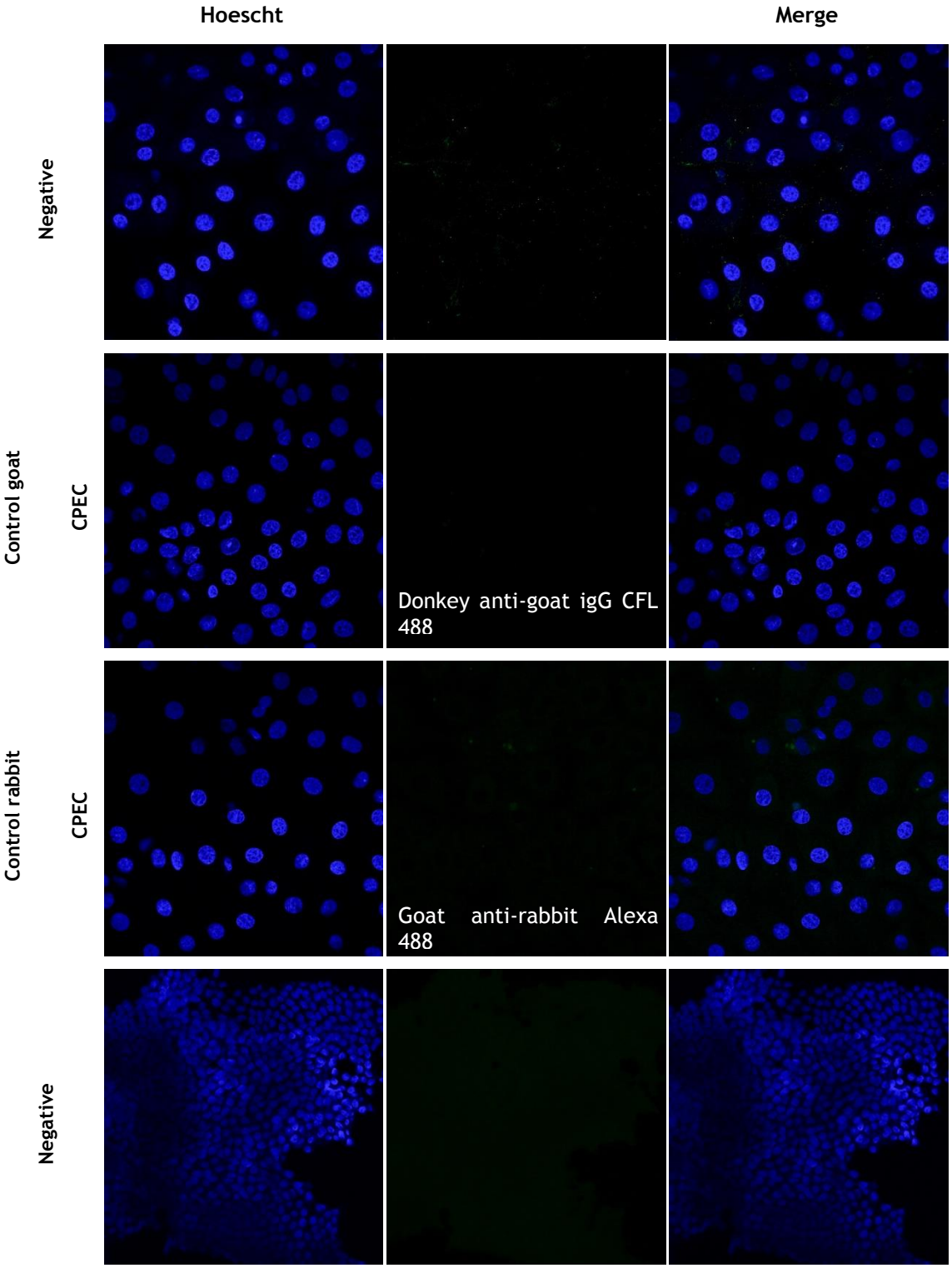
Hoescht
Merge
Negative
Control goat
CPEC
Donkey anti-goat igG CFL 488
Control rabbit
CPEC
Goat anti-rabbit Alexa 488
Negative

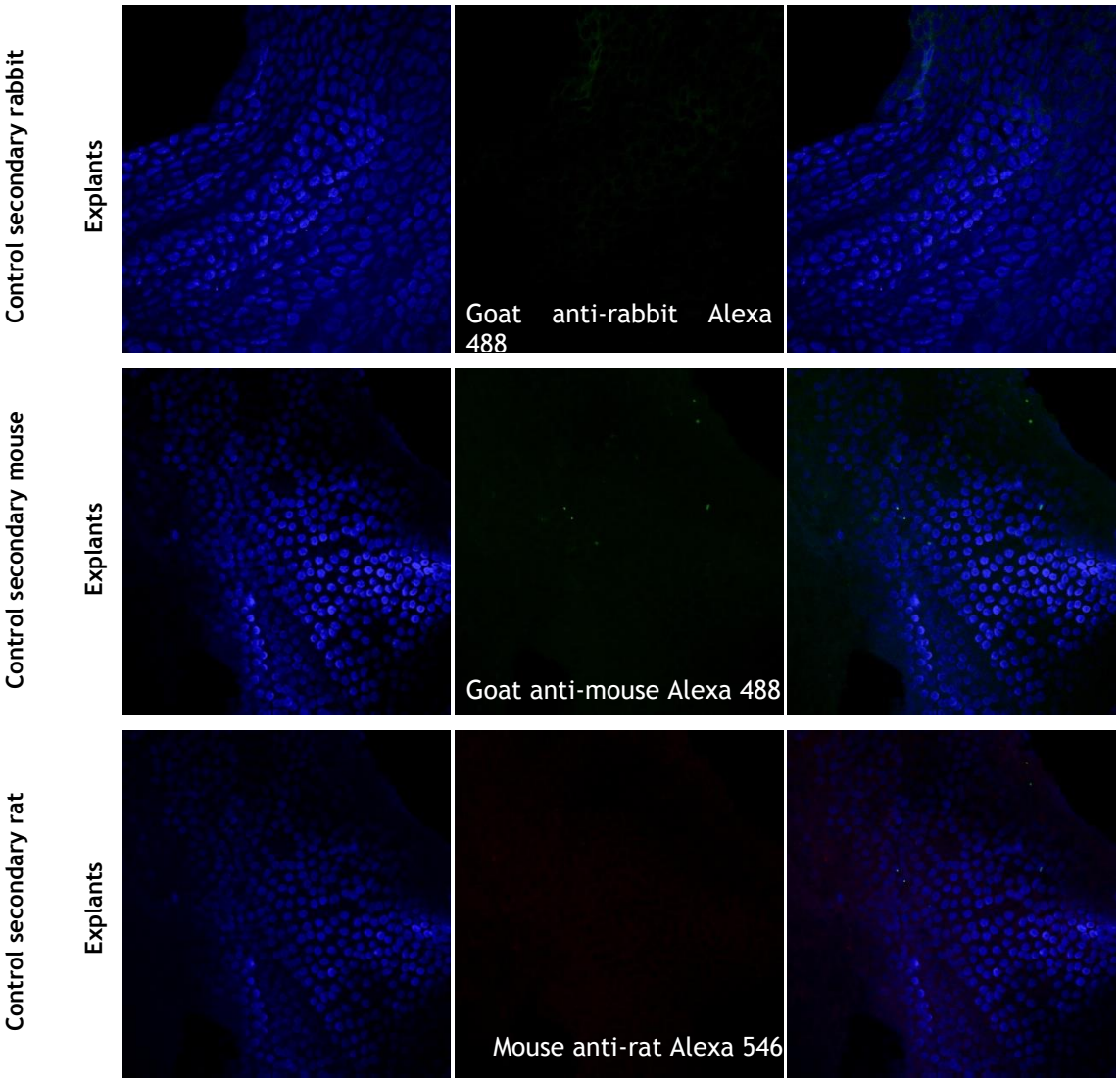
Control secondary rabbit
Explants
Goat anti-rabbit Alexa 488
Control secondary mouse
Explants
Goat anti-mouse Alexa 488
Control secondary rat
Explants
Mouse anti-rat Alexa 546